SSSTJ
VOL.7 NO.1
January2020
ISSN 2351-0889

SSSTJ

Suan Sunandha Science and Technology Journal

Volume 7, Number 1, January 2020

Suan Sunandha Science and Technology Journal

General Information

The Suan Sunandha Science and Technology Journal (SSSTJ) is a double-blind peer reviewed scientific journal published twice a year (January and July) by the Faculty of Science and Technology, Suan Sunandha Rajabhat University. Submissions of manuscripts should be sent to the Editor of the SSSTJ by online system: http://www.ssstj.sci.ssru.ac.th. The manuscript will be taken that all contributing authors attest that manuscripts and material submitted to the SSSTJ are original and have not been published or submitted elsewhere and the authors concede to the open-access distribution of the manuscript, including all contents contained therein.

Aim and scope:

Suan Sunandha Science and Technology Journal (SSSTJ) is an international academic journal that gains foothold at Suan Sunandha Rajabhat University, Thailand and opens to scientific communications in Southeast Asia, Asia and worldwide. It aims to contribute significant articles in science and technology researches. Published papers are focused on state of the art science and technology. Committee of the journal and association will review submitted papers. The authors may include researchers, managers, operators, students, teachers and developers.

Following areas are considered for publication:
1. Applied Physics
2. Applied Statistics
3. Biology
4. Biotechnology
5. Chemistry
6. Computer Science
7. Energy
8. Environmental Science and Technology
9. Information Technology
10. Mathematics
11. Microbiology
12. Food Science and Technology
13. Forensic Science
14. Sport Science
15. Other related fields

QR CODE Journal

Suan Sunandha Science and Technology Journal

Editorial Board

SUAN SUNANDHA SCIENCE AND TECHNOLOGY JOURNAL
Suan Sunandha Rajabhat University, Faculty of Science and Technology
1 U-thong Nok Road, Dusit, Bangkok 10300 THAILAND

CONTENTS

Volume 7, No.1 **January 2020**

Available online at http://www.ssstj.sci.ssru.ac.th

Suan Sunandha Science and Technology Journal

Synthesis and Evaluation of Molecularly Imprinted Polymer As a Selective Material for Vanillin

Thitiporn Pengkamta[1], Molthicha Mala[1], Chanapa Klakasikit[1], Patcharawan Kanawuttikorn[1], Pornanan Boonkorn[2], Angkana Chuaejedton[2], Weeranuch Karuehanon[1,*]

[1]Chemistry Program and Center of Excellence for Innovation in Chemistry, Faculty of Science, Lampang Rajabhat University, Lampang 52100, Thailand

[2]Biology Program, Faculty of Science, Lampang Rajabhat University, Lampang 52100, Thailand

Corresponding author e-mail: * w.karuehanon@lpru.ac.th

Received: *18 December 2019* / **Revised:** *31 December 2019* / **Accepted:** *7 January 2020*

Abstract

Molecularly imprinted polymers (MIPs) using vanillin (Val) as a template molecule were synthesized and evaluated. MIPs were prepared by precipitation polymerization using various types of functional monomers with using ethylene glycol dimethacrylate (EGDMA) and trimethylolpropane trimethacrylate (TRIM) as cross linkers and polymerization was done at 80°C for 6 h. The binding efficiency of polymers was evaluated including types of monomers, binding time and reusability. Results showed that methacrylic acid was the selective monomer for vanillin and the highest performance of MIPs, which including the binding efficiency and selectivity, was obtained when bound polymer with vanillin for only 2 h and could be reused as least five times.

Keywords: Vanillin, Molecularly imprinted polymer, Selective material

1. Introduction

Molecularly imprinted polymers (MIPs) are a very attractive materials in various fields, including separation (Hong & Chen, 2013), purification (Mokgadi, Batlokwa, Mosepele, Obuseng, & Torto, 2013), sensors (Lee, Oh, Kim, & Jang, 2015), pharmaceutical (Diouf, Motia, El Alami El Hassani, El Bari, & Bouchikhi, 2017) and catalysts (Wulff, 2002). The composition of this materials are template molecule (or target molecule), functional monomer, cross-linker and initiator. Generally, the preparation of MIPs include 3 steps which are self-assembly, polymerization and template removal (Mayes & Whitcombe, 2005). Firstly, self-assembly was done by interacted template molecule with functional monomer which can be covalent or non-covalent interaction then cross-linker and initiator are added for polymerization reaction. After polymerization, polymer which contains template molecule can be obtained. Finally, to create imprinted polymer, the template is removed from polymer using suitable solvent extraction method to leave the cavity of template inside the polymer which exhibited high template recognition affinity.

Vanillin (Val) is the valuable compound in food industry which provide as an ingredient in wide range such as food flavor, beverage, pharmaceutical and perfume (Esposito et al., 1997). This compound can be originally obtained from a seed of vanilla which is a very unique and highly prize compound due to its various applications (Mohamad Ibrahim, Sipaut, & Mohamad Yusof, 2009). Other natural source of vanillin is extracted from softwood lignin by catalytic decomposition (Borges da Silva et al., 2009) and recrystallization method which are very expensive process and high amount of impurities will be occurred (Wu et al., 2015). Solid-phase extraction (SPE) with solid-sorbent such as C18 or ion-exchange resin has generally applied for purification of interested compounds. However, the high cost sorbent materials with cannot be reused and non-selective extraction and have been observed (Xu, Yang, & Liu, 2014), therefore, high selective materials with low cost production and reusable are still promising.

In present study, we have synthesized and evaluated molecularly imprinted polymer selective to vanillin (MIP-Val) with various types of functional monomers and cross-linkers. The binding

Suan Sunandha Science and Technology Journal

study with template molecule was applied to indicate the efficiency of MIP-Val and the effect of types of polymers, binding time and reusability were investigated.

2. Materials and Methods

2.1 Synthesis of molecularly imprinted polymer for vanillin (MIP-Val)

All polymers were synthesized according to the literature report (Karuehanon, Wongthep, & Wanggnorn, 2018). For MIPs-Val synthesis, in 150 ml round-bottom flask, vanillin 0.25 mmol and functional monomer 1 mmol were added and dissolved in 25 ml of acetonitrile. After incubated the solution for 15 min, 5 mmol of cross-linker was added following by 0.125 mmol of benzolyl peroxide and 25 ml of acetonitrile, solution was then stirred at room temperature for 5 min before bubbled with N_2 gas for 15 min. The precipitation polymerization was carried out at 80˚C for 6 h and washed the obtained polymer with acetonitrile. Template extracting step was done by stirring synthesized polymers in 100 ml off methanol:acetic acid solution (8:2 v/v) for 2 h x 5 times until no trace of vanillin was observed by UV-Visible spectrophotometer (λ_{max}= 274 nm) then washed with distilled water until pH of washing solution was neutral following by acetonitrile and acetone before dried in hot air oven at 80˚C, overnight. Non-Imprinted polymers (NIPs) were synthesized using the same procedure with MIPs in the absence of vanillin. The yield of synthesized MIPs was calculated according to equation (1).

$$\%Yield_{MIP} = \frac{W_{MIP}}{W_m + W_c} \times 100 \qquad (1)$$

When

W_{MIP} is weight of synthesized MIP after template removal (mg)

W_m is weight of functional monomer used in synthesis (mg)

W_c is weight of cross-linker used in synthesis (mg)

2.2 Binding study of MIP-Val

The binding study of synthesized MIP-Vals and its corresponding NIPs was done by re-binding polymers with vanillin solution (template molecule). In 1.5 ml of micro centrifuge tube, 5 mg of polymer and 1 ml of vanillin in concentration of 10 ppm were added then carefully close the cap and wrap with parafilm. All prepared tubes were then incubated with the shaking incubator at room temperature with investigated binding time then centrifuged at 6,000 rpm for 5 min. The supernatant was then separated to another micro centrifuge tube and the absorbance of vanillin was determined using UV-Visible spectrophotometer at λ_{max}= 274 nm. The concentration of vanillin in supernatant was then calculated from calibration curve of vanillin ($y=0.0385x+0.0325$, $R^2=1$). %Bound and imprinting factor (α) of polymer was calculated following equation (2) and (3) which indicated efficiency of re-binding and selectivity of polymer (Karuehanon, Lee, Nimmanpipug, Tayapiwatana, & Pattarawarapan, 2009), respectively.

$$\%Bound = \frac{Q_0 - Q}{Q_0} \times 100 \qquad (2)$$

When

Q_0 is initial concentration of vanillin before binding with polymer (ppm)

Q is concentration of vanillin in supernatant after binding with polymer (ppm)

$$\alpha = \frac{\%Bound_{MIP}}{\%Bound_{NIP}} \qquad (3)$$

When

$\%Bound_{MIP}$ is %Bound of MIP

$\%Bound_{NIP}$ is %Bound of corresponding NIP

2.3 Reusability of MIP-Val

The reusability of MIP was observed with the selected polymer which showed the highest performance of binding study. Vanillin solution (10 ppm) was added to selected MIP in ratio of MIP:vanillin as 5 mg : 1 ml. Firstly, the binding study was done as described method with 50 mg of MIP in 10 ml of vanillin solution for the first cycle. After analyzed the supernatant by UV-Visible spectrophotometer, the left MIP was then washed with 100 ml of methanol:acetic acid solution (8:2 v/v) for 2 h x 5 times to remove vanillin from MIP and washed with water, acetonitrile and acetone, espectively, before dried by hot air oven. The prepared MIP was then weighted as 40 mg for second cycle of binding study with 8 ml of vanillin solution (as previously ratio of MIP:vanillin as 5 mg : 1 ml) due to prevent the loss of MIP during template removal and washing step which recovered less than 50 mg. And the reusability was continued to fifth cycle with using 30, 20 and 10 mg of MIP with 6, 4 and 2 ml of vanillin solution, respectively

Vol.07, No.1 DOI: 10.14456/ssstj.2020.2

Suan Sunandha Science and Technology Journal

3. Results and Discussions

3.1 Synthesis of MIPs

Six types of functional monomer, including methacrylic acid (MAA), 2-hydroxyethyl acrylate (HEA), methyl methacrylate (MMA), acrylamide (ACM), 4-vinylpyridine (4VP) and N,N-methylene bis acrylamide (MBA), with two types of cross-linkers; ethylene glycol dimethacrylate (EGDMA) and trimethylolpropane trimethacrylate (TRIM), were used for synthesis (Figure 1). All MIPs using vanillin as a template molecule and their corresponding NIPs were synthesized by precipitation polymerization method. All polymers were obtained as white powder and the %yield was showed in Table 1.

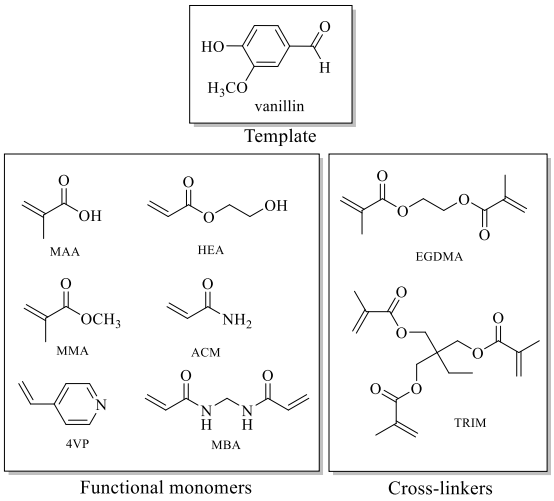

Figure 1. Structure of vanillin, functional monomers and cross-linkers used in this study.

From results showed in Table 1., %Yield of synthesized polymer was in the rage of 17.63 – 90.50% for using EGDMA as cross-linkers (entry 1 – 6) and 57.67 – 98.88% which less than when using TRIM as a cross-linkers (entry 7 – 12). Since TRIM has three branch chain containing three vinyl group (–CH=CH$_2$) in molecule, this can be favorable structure for the polymerization more than EGDMA which contains only two vinyl groups in structure. For considering the effect of types of functional monomers to the yield of polymer, three types of functional monomers including acidic (MAA), neutral (HEA and MMA) and basic (ACM, 4VP and MBA) were applied in this study. The lowest yield of MIPs prepared by using 4VP, strong organic base monomer, were observed in both of cross-linkers (entry 5, 11). This could be due to the weak interaction between vanillin and nitrogen atom in structure of vinylpyridine. On the other hand, acidic monomer as MAA (entry 1, 7) exhibited the highest %yield of MIPs in both of cross-linkers, since MAA which contains carboxylic group (–COOH) has demonstrated H-bonding interaction with template molecule among others monomers (Figure 2) (Mohamad Ibrahim et al., 2009). Moreover, it was found that most of prepared NIPs were achieved in higher yield than MIPs. This could be caused by the synthetic process which NIPs could be prepared by only polymerization step while the synthesis of MIPs initiated by self-assembly step before polymerization, which binding interaction between monomer and template was the major effect to the completion of polymerization reaction.

Table 1. Synthesis of MIPs.

Entry	Functional monomer	Cross-linker	%Yield	
			MIP	NIP
1	MAA	EGDMA	65.17	67.68
2	HEA	EGDMA	38.29	90.50
3	MMA	EGDMA	38.30	69.43
4	ACM	EGDMA	46.41	83.13
5	4VP	EGDMA	17.63	85.08
6	MBA	EGDMA	53.61	88.45
7	MAA	TRIM	98.88	94.10
8	HEA	TRIM	73.96	93.42
9	MMA	TRIM	97.40	80.13
10	ACM	TRIM	87.34	57.67
11	4VP	TRIM	64.86	78.25
12	MBA	TRIM	80.05	88.16

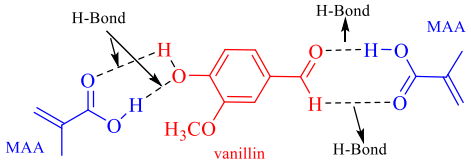

Figure 2. Binding interaction between vanillin and MAA.

3.2 Binding study of MIPs

The efficiency of MIPs was investigated by binding study which re-bound vanillin to MIPs and their corresponding NIPs. %Bound and imprinting factor (α) indicated the binding affinity and selectivity of MIPs which calculated as previously describe. Firstly, 12 types of synthesized polymer according to Table 1 were investigated with using 5 mg polymers bound with 1 ml of vanillin solution (10 ppm), for 24 h at room temperature. Results of binding study were shown in Figure 3 (a) and Figure 3 (b) for using EGDMA and TRIM as cross-linkers, respectively. Surprisingly, non-selective binding was observed in the most of polymers that could be

Vol.07, No.1 DOI: 10.14456/ssstj.2020.2

Suan Sunandha Science and Technology Journal

shown by the low value of imprinting factor (α nearly or less than 1) which indicated that NIPs showed higher binding affinity than MIPs, since NIPs were synthesized by the absences of vanillin and had no cavity inside polymer. However, MIPs synthesized by MAA in both of cross-linkers showed good binding efficiency to template molecule with imprinting factor value as 1.76 (%Bound = 34.45) and 1.93 (%Bound = 31.78) for EGDMA and TRIM, respectively. This would be caused by the strong binding interaction between the cavities inside MIPs with functionalized by carboxylic acid of MAA as shown in Figure 2, therefore, these two types of MIPs and their corresponding NIPs were selected for further study.

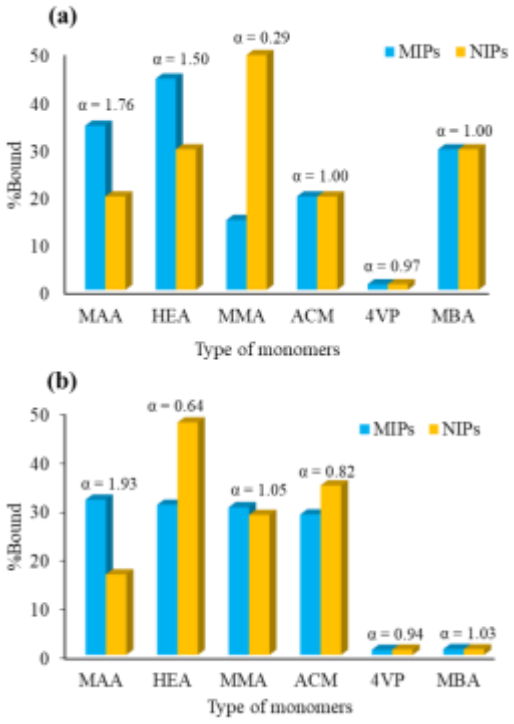

Figure 3. Binding affinity of polymers synthesized by using (a) EGDMA and (b) TRIM as a cross-linker.

3.3 Effect of binding time

Two types of polymer using MAA as a functional monomer with EGDMA and TRIM as a cross-linkers were then selected to study the effect of binding time. The binding experiments were also done by previously procedure with varied incubation time as 1, 2, 4, 6, 12 and 24 h at room temperature. Results in Figure 4 showed the uncertainly %Bound of NIPs when increasing of time which could be explained by non-specific binding, the binding interaction was only occurred at the surface of NIPs (Kantarovich, Belmont, Haupt, Bar, & Gheber, 2009). For MIPs, high %Bound was observed from both of polymers from 1 h of binding time then slightly decreased when increasing of time before increased and stabled. This binding behavior attributed by the rebinding of template at the cavities created from self-assembly process and binding equilibrium (Ansell, 2015). Nevertheless, very high imprinting factor value as 6.21 (41.87%Bound) and 4.11 (46.88%Bound) were showed in both MIPs with binding time as 2 h. Although for MAA-TRIM at 1h (Figure 4 (b)), the highest %Bound of MIP (51.06%) was obtained but imprinting factor was two times lower than at 2 h. Therefore, as the moderate affinity in which of both %Bound and imprinting factor value, MIPs using MAA-EDMA and MAA-TRIM synthesis system showed the highest performance when bound with template for 2 h and this protocol was selected to study the reusability of MIPs.

Figure 4. The effect of binding time of MIP-Val

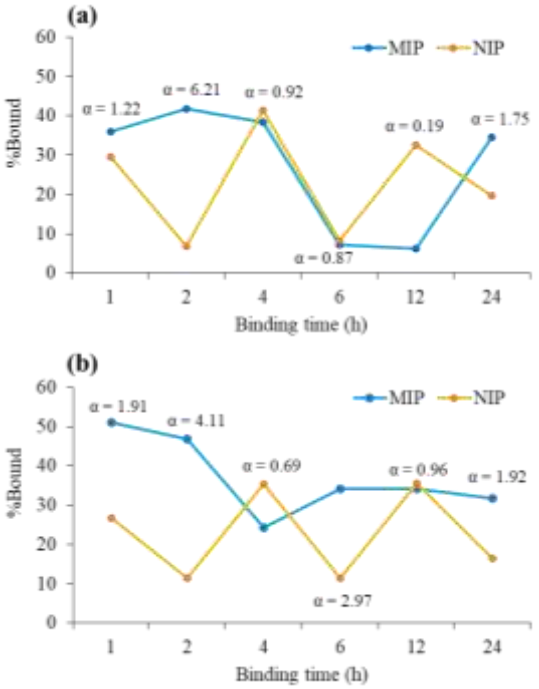

synthesized by (a) MAA-EGDMA and (b) MAA-TRIM.

3.4 Reusability of MIPs

The reusability of MAA-EGDMA and MAA-TRIM were studied in five cycles for binding with

Vol.07, No.1 DOI: 10.14456/ssstj.2020.2

Suan Sunandha Science and Technology Journal

10 ppm of vanillin for 2 h and results showed in Figure 5. The ratio between MIP:vanillin solution was 5 mg:1 ml and all MIPs were scaled-up to 50 mg in the first cycle to prevent the losing of MIPs during study in five cycles. It could be seen that MAA-TRIM showed higher %Bound than MAA-EGDMA and %Bound of MIPs were slightly decreased when continuously reused from first cycle to fifth cycles which was from 42.10% to 37.56% for MAA-EGDMA and 47.22% to 45.12% for MAA-TRIM, respectively. However, these MIPs could be reused at least five times with less than 5% of %Bound decreasing.

Figure 5. Reusability of MAA-EGDMA and MAA-TRIM

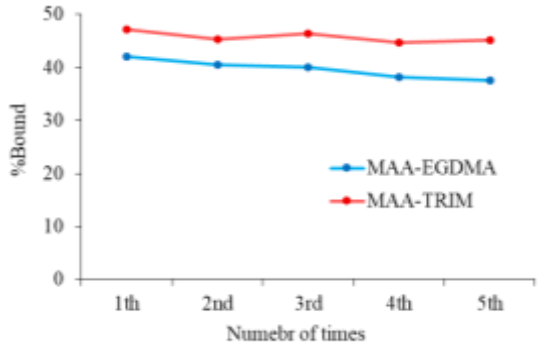

4. Conclusion

Molecularly imprinted polymers (MIPs) selective to vanillin were synthesized using various types of functional monomer and cross-linkers by precipitation polymerization. The binding efficiency of synthesized MIPs were evaluated with various effects including types of polymers, binding time and reusability. Methacrylic acid (MMA) was the suitable functional monomer for synthesis of MIPs using vanillin as a template molecule. Both of ethylene glycol dimethacrylate (EGDMA) and trimethylolpropane trimethacrylate (TRIM) could be used as cross-linkers to achieve the highest performance of MIPs with high binding affinity and high selectivity at 2 h of binding time. Moreover, the studied MIPs could be reused at least five times with moderate affinity compare with first time usage.

5. Acknowledgement

The authors would like to thank Center of Excellence for Innovation in Chemistry (PERCH-CIC) for providing facilities. The financial and facilities support from Faculty of Science, Lampang Rajabhat University is also gratefully appreciated.

6. Publication Ethic

Submitted manuscripts must not have been previously published by or be under review by another print or online journal or source

7. References

Ansell, R. J. (2015). Characterization of the binding properties of molecularly imprinted polymers. *Advances in Biochemical Engineering/Biotechnology*, *150*, 51-93.

Borges da Silva, E. A., Zabkova, M., Araujo, J. D., Cateto, C. A., Barreiro, M. F., Belgacem, M. N., & Rodrigues, A. E. (2009). An integrated process to produce vanillin and lignin-based polyurethanes from Kraft lignin. *Chemical Engineering Research and Design*, *87*(9), 1276-1292.

Diouf, A., Motia, S., El Alami El Hassani, N., El Bari, N., & Bouchikhi, B. (2017). Development and characterization of an electrochemical biosensor for creatinine detection in human urine based on functional molecularly imprinted polymer. *Journal of Electroanalytical Chemistry*, *788*, 44-53.

Esposito, L. J., Formanek, K., Kientz, G., Mauger, F., Maureaux, V., Robert, G., & Truchet, F. (1997). Vanillin. In *Kirk-Othmer Encyclopedia of chemical technology*. New Jersey: John Wiley & Sons.

Hong, Y., & Chen, L. (2013). Extraction of quercetin from Herba Lysimachiae by molecularly imprinted-matrix solid phase dispersion. *Journal of Chromatography B*, *941*, 38-44.

Kantarovich, K., Belmont, A. S., Haupt, K., Bar, I., & Gheber, L. A. (2009). Detection of template binding to molecularly imprinted polymers by Raman microspectroscopy. *Applied Physics Letters*, *94*, 194103.

Karuehanon, W., Lee, V. S., Nimmanpipug, P., Tayapiwatana, C., & Pattarawarapan, M. (2009). Synthesis of molecularly imprinted polymers for nevirapine by dummy template imprinting approach. *Chromatographia*, *70*, 1531-1537.

Karuehanon, W., Wongthep, T., & Wanggnorn, C. (2018). Synthesis of molecularly imprinted polymers for extraction of quercetin from mulberry leaves. *Prawarun Agricultural Journal*, *15*, 96-103.

Lee, J. S., Oh, J., Kim, S. G., & Jang, J. (2015). Highly sensitive and selective field-effect-transistor nonenzyme dopamine sensors

Suan Sunandha Science and Technology Journal

based on Pt/conducting polymer hybrid nanoparticles. *Small*, *11*, 2399-2406.

Mayes, A. G., & Whitcombe, M. J. (2005). Synthetic strategies for the generation of molecularly imprinted organic polymers. *Advanced Drug Delivery Reviews*, *57*(12), 1742-1778.

Mohamad Ibrahim, M. N., Sipaut, C. S., & Mohamad Yusof, N. N. (2009). Purification of vanillin by a molecular imprinting polymer technique. *Separation and Purification Technology*, *66*, 450-456.

Mokgadi, J., Batlokwa, S., Mosepele, K., Obuseng, V., & Torto, N. (2013). Pressurized hot water extraction coupled to molecularly imprinted polymers for simultaneous extraction and clean-up of pesticides residues in edible and medicinal plants of the Okavango Delta, Botswana. *Molecular Imprinting*, *1*, 55-64.

Wu, J., Yang, Z., Chen, N., Zhu, W., Hong, J., Huang, C., & Zhou, X. (2015). Vanillin-molecularly targeted extraction of stir bar based on magnetic field induced self-assembly of multifunctional Fe_3O_4@ Polyaniline nanoparticles for detection of vanilla-flavor enhancers in infant milk powders. *Journal of Colloid and Interface Science*, *442*, 22-29.

Wulff, G. (2002). Enzyme-like catalysis by molecularly imprinted polymers. *Chemical Reviews*, *102*, 1-27.

Xu, Z., Yang, Z., & Liu, Z. (2014). Development of dual-templates molecularly imprinted stir bar sorptive extraction and its application for the analysis of environmental estrogens in water and plastic samples. *Journal of Chromatography A*, *1358*, 52-59.

Available online at http://www.ssstj.sci.ssru.ac.th

Suan Sunandha Science and Technology Journal

The Effect of Extraction Methods on Phenolic, Anthocyanin, and Antioxidant Activities of Riceberry Bran

Supatchalee Sirichokworrakit[1*], Hathairat Rimkeeree[1], Withida Chantrapornchai[1], Udomluk Sukatta[2], Prapassorn Rugthaworn[2]

[1] Department of Product Development, Faculty of Agro-Industry, Kasetsart University
50 Ngam Wong Wan Rd, Latyao, Chatuchak, Bangkok 10900, Thailand
[2] Kasetsart Agicultural and Agro-Industrial Product Improvement Institute, Kasetsart University
50 Ngam Wong Wan Rd, Latyao, Chatuchak, Bangkok 10900, Thailand
Corresponding author e-mail: *supatchalee.siri@gmail.com
Received*: 18 December 2019* / **Revised:** *31 December 2019* / **Accepted:** *7 January 2020*

Abstract

Riceberry bran, byproduct from the rice milling process, is one of bioactive compounds sources. In order to increase Riceberry bran value, the purpose of this study was to compare the effect of different Riceberry bran extraction methods, including accelerated solvent extraction (ASE), ultrasonic-assisted extraction (UAE), soxhlet extraction (SE), and maceration method (MC) on bioactive compounds and antioxidant activities. It was found that the Riceberry bran extract from ASE presented the highest total phenolic, total anthocyanin content (55.45 mg GAE/g and 3.06 mg/g) and antioxidant properties including IC_{50} of DPPH assay (0.109 mg/mL), FRAP value (688.04 mmole Fe(II)/kg) and IC_{50} of ABTS assay (3.42 mg/mL) among the four methods. These results imply the potential to use the ASE method for extraction of phenolic and anthocyanin compounds from Riceberry bran.

Keywords: Accelerated solvent extraction, Maceration, Riceberry bran, Soxhlet, Ultrasonic-assisted extraction

1. Introduction

Riceberry, deep purple grain; (*Oryza sativa* L.), a cross-bred strain from the Khao Hom Nin Rice variety which is well known as containing high antioxidant properties and Khao Hom Mali 105 well known as fragrant rice (Leardkamolkarn et al., 2011). Consumption of Riceberry is becoming popular in Thailand because of high nutrition and so as to meet the increasing market demand, the Thai government is supporting farmers to grow Riceberry (Peanparkdee, Yamauchi, & Iwamoto, 2018). Riceberry bran is a byproduct of the rice milling process. It is always extracted oil and defatted Riceberry bran is used an ingredient in animal feed. A number of studies have reported the presence of bioactive compounds in Riceberry bran. For instance, Riceberry bran is a rich source of phenolic compounds, anthocyanins, vitamin E and oryzanol which have shown great antioxidant activities (Peanparkdee et al., 2018). In addition, several studies reported that Riceberry possessed chemopreventive properties including decreasing inflammation, managing diabetes and improving the regenerative changes of the pancreas, kidneys, heart and liver (Leardkamolkarn et al., 2011; Posuwan et al., 2013; Prangthip et al., 2013). Extraction, the first step of bioactive compounds study, plays a significant and important role in the final quality of the extract. There are many extraction techniques that have been developed for the extraction of bioactive components from rice bran such as UAE, ASE microwave and ohmic heating-assisted extraction, etc. Peanparkdee et al. (2018) extracted phenolic and anthocyanins from Riceberry bran using UAE. Suttiarporn, Sookwong, and Mahatheeranont (2016) studied fractionation and identification of antioxidant compounds from Riceberry bran using solvent extraction (hexane, dichloromethane and methanol). However, there is little published information to compare extraction methods of bioactive compound from Riceberry bran. Conventional solvent extraction is used in extracting bioactive compounds from plants, based on many parameters, including the amount of solvents, extraction time, polarity of the antioxidant, and temperature (Peanparkdee et al., 2018). The conventional methods such as SE, and MC are still considered to be compared with new

Suan Sunandha Science and Technology Journal

extraction methods. Recently, new extraction methods have obtained increasing attentiveness to produce more environmentally sustainable, more effective, decreasing cost and faster extraction (Barros, Dykes, Awika, & Rooney, 2013). New extraction methods were used in various bioactive compounds, such as phenolic from rice bran (Tabaraki & Nateghi, 2011) using UAE since it can increase the efficiency of solvent extraction. ASE was also used to extract phenolic compounds from sorghum brans (Barros et al., 2013), and anthocyanin composition from blue wheat, purple corn, and black rice (Abdel-Aal, Akhtar, Rabalski, & Bryan, 2014). This method uses a combination of elevated temperature and pressure with common solvents to increase the efficiency of the extraction process. The result is faster run times and a significant reduction in solvent use. Therefore, the main objective of the present study was to extract Riceberry bran using ASE, UAE, SE, and MC followed by the evaluation of the total phenolic content, total anthocyanin content and antioxidant activities in order to increase the utilization of Riceberry bran.

2. Methodology

2.1 Raw material

Defatted Riceberry bran (*Oryza sativa* L.) obtained from Sunfood Corp Limited (Samutprakan, Thailand). It was sieved through 20–100 mesh screen. It was kept in a sealed container at -18°C. All measurements were performed in triplicate.

2.2 Chemicals

Folin-Ciocaltue reagent gallic acid, 2,2'-azaino-bis (3-ethylbenzothiazoline-6-sulfonic acid) diammonium salt (ABTS), 2,2'-dipheny-l-picrylhydrazyl (DPPH), , ascorbic acid (vitamin C), α-tocopherol and 2,6-di-tert-butyl-4-methyl-phenol were purchased from Sigma-Aldrich (St. Louis, MO). Potassium chloride and sodium carbonate were purchased from Ajax Finechem (NSW, Australia). Sodium acetate hydrate and furrous sulphate were purchased from Carlo Erba (Chaussee du Vexin, France). Hydrochloric acid was purchased from Merck (Darmstadt, Germany).

2.3 Determination of extract yield

The yield of extracts on a dry weight basis was calculated from equation (1) as shown below:

$$\text{Extract yield (\%)} = (W_1 \times 100) / W_2 \quad (1)$$

W_1 was the weight of extract after evaporation of ethanol
W_2 was the dry weight of the fresh plant sample

2.4 Determination of moisture content

The moisture content of the Riceberry bran was analyzed according to AOAC methods (Association of Official Analytical Chemists [AOAC], 2019).

2.5 Determination of water activity (a_w)

a_w was determined at 25°C using a_w meter, Aqua Lab (Series 3 TE (Decagon Devices Inc., USA). Approximately 2 g of the ground sample was used for the analysis.

2.6 Determination of color value

The color of rice bran was measured with spectrophotometer (Hunter Lab, Color Quest XE, USA) equipped with a D65 illuminant using the CIE L* a* b* system.

2.7 Sample extraction

Four extraction methods, ASE, UAE, SE, and MC were investigated. Riceberry bran was extracted with ethanol using UAE method according to Tabaraki and Nateghi (2011) method with some modifications. The bran (10 g) was dissolved in 200 mL of 67% (v/v) aqueous ethanol. The sample was sonicated (37 kHz) in an ultrasonic cleaner (Ultrasonic bath, Elama siries Elmasonic P, Germany) at 55°C for 40 min. The resulting extract was filtered through a Whatman No.1 filter paper and vacuum-dried in a rotary evaporator (Rotavapor R-100, Buchi, Switzerland) at 40°C. The crude extract was stored at -18ºC until use.

ASE was performed on a Dionex ASE 350 system (Thermo Scientific, USA). The bran sample of 10 g was mixed with diatomaceous earth (DE) in a proportion of 1:1 and placed in a 66 mL stainless steel extraction cell. A cellulose D28 filter (Dionex Corporation) was placed at the bottom of the extraction cell to avoid the collection of suspended particles in the collection vial. The extraction cells

Vol.07, No.1 DOI: 10.14456/ssstj.2020.1

Suan Sunandha Science and Technology Journal

were arranged in the sample carousel and prefilled with the solvent (67% ethanol), static time 10 min, and heated at 55°C. The extraction was done using 5 cycles and the cell was rinsed with 100% flush. The extract was collected in 250 mL collection vials. The resulting extract was filtered through a Whatman No. 1 filter paper and vacuum-dried in a rotary evaporator at 40°C. The crude extract was stored at -18ºC until use.

The SE was based on the UAE method. The bran (10 g) was placed in a thimble and put it in the extractor that dissolved in 50 mL of 67% ethanol. The distillation flask was filled with 250 mL of 67% ethanol, and heat source. The sample was placed in a thimble-holder that was gradually filled with condensed fresh extractant from a distillation flask. When the solvent reached the overflow level, a siphon aspirates the solute from the thimble-holder and unloaded it back into the distillation flask, thus carrying the extracted analyses into the bulk liquid. This operation was repeated until the solvent in the extractor was clear. The resulting extract was filtered through a Whatman No.1 filter paper and vacuum-dried in a rotary evaporator at 40°C. The crude extract was stored at -18ºC until use.

MC was investigated at room temperature. The bran (10 g) was dissolved in 200 mL of 67% ethanol in closed bottles. After 48 h of extraction, the extract was filtered through a Whatman No. 1 filter paper and repeat 3 times until the extract was clear. The collection of the extract was vacuum-dried in a rotary evaporator at 40°C. The crude extract was stored at -18ºC until use.

2.8 Determination of total phenolic content

The total phenolic content of Riceberry bran extracts was determined by the Folin-Ciocalteu reagent using different concentration (0-200 µg/mL) of Gallic acid as standard (Wolfe, Wu, & Liu, 2003) with some modifications. 125 µL of samples were mixed with 500 µL distilled water in a test tube followed by the addition of 125 µL of Folin-Ciocalteu reagent and allowed to stand at room temperature for 6 min. Then it was mixed with 1,250 µL of 7% Na_2CO_3 and followed by the addition of 1,000 µL of distilled water and allowed to stand at room temperature for 90 min. The absorbance of the mixtures was determined at 760 nm in spectrophotometer (UV mini-1240, Shimadzu, USA). Total phenolic content in the extract was expressed in mg Gallic acid equivalent/g.

2.9 Determination of anthocyanin content

The analysis method for anthocyanin content was modified from the method used by Giusti & Wrolstad (2005). The Riceberry bran extracts (1 mL) in 25 mL of volume metric flasks were adjusted with potassium chloride buffer (0.03 mol/L, pH 1.0) and the other was adjusted with sodium acetate buffer (0.4 mol/L, pH 4.5). Each of them was left for 15 min in the dark at room temperature. The absorbance of the mixtures was determined at 510 nm and 700 nm in spectrophotometer. The anthocyanin concentration (mg/L) of sample was calculated according to the following formula (2) and expressed as Cyanidin-3-glucoside equivalents:

Total anthocyanin content (mg/g) = (A x MW x DF x V) / (ε x 1 x G) (2)

A was $(A\lambda_{700} - \lambda_{510})$ pH 1.0 - $(A\lambda_{700} - \lambda_{510})$ pH 4.5
MW was the molecular weight of Cyanindin-3glu coside (449.2 g/mol)
DF was the dilution factor (20 µL sample is diluted to 2 mL, DF = 1000)
ε was the extinction coefficient (L × cm-1 × mol-1) = 26,900 for Cyanindin-3-glucoside where L (path length in cm) = 1
l was the volume of solvent
G was the weight of sample

2.10 Determination of antioxidant activities

- IC_{50} of DPPH scavenging activity

The free radical scavenging activity of Riceberry bran extracts will be evaluated using the stable radical DPPH according to the method of Re et al. (1999). Various concentration of each extract was pipetted into 1 mL DPPH working solution. The mixture was shaken and incubated for 30 min in the dark at room temperature. Ascorbic acid, α-tocopherol, and BHT were used as standard. The analysis was done in triplicate for standard and each extract. The absorbance of the mixtures was determined at 517 nm relative to the control (as 100%) using a spectrophotometer. The percentage of radical scavenging ability was calculated by using the formula (3):

Vol.07, No.1 DOI: 10.14456/ssstj.2020.1

Suan Sunandha Science and Technology Journal

Scavenging ability (%) =

$$\frac{(\text{Absorbance 517 nm of control} - \text{Absorbance 517 nm of sample}) \times 100}{\text{Absorbance 517 nm of control}} \quad (3)$$

IC_{50} of DPPH scavenging activity of each extract could be calculated using its calibration curve.

- Ferric reducing antioxidant power (FRAP)

The FRAP assay was modified from Benzie and Strain (1999). 60 µL of samples were mixed with 1.8 mL of the FRAP reagent and 180 µL of distilled water. The absorbance of the mixtures was determined at 593 nm using a spectrophotometer after 4 min incubation at 37°C. FRAP reagent was prepared daily and consisted of 0.3 M acetate buffer (pH 3.6), 10 mM TPTZ in 40 mM HCl, 20 mM $FeCl_3$ and distilled water in a ratio of 10:1:1:1.2 (v/v/v/v). FRAP value was obtained by comparing the absorbance change in the test mixture with doses obtained from increasing concentrations of Fe(III) and expressed as mmol of Fe(II) equivalents per g extract. Ascorbic acid, α-tocopherol, and BHT were used as standard.

- IC_{50} of ABTS radical scavenging assay

ABTS radical scavenging activity was determined according to Re et al. (1999) with some modification. A stable stock solution of ABTS radical cation was produced by reacting a 7 mM aqueous solution of ABTS with potassium persulfate in the dark at room temperature for 12-16 h before use. The working solution was diluted with 95% ethanol to reach and absorbance of 0.7±0.02 at 734 nm. 20 µL of samples were mixed with 2 mL of working solution, and the absorbance was measured immediately at 734 nm after 6 min at room temperature in the dark. Ascorbic acid, α-tocopherol, and BHT were used as standard. The analysis was done in triplicate for standard and each sample. Antioxidant capacity of each sample was determined based on the reduction of ABTS absorbance by calculating the percentage of antioxidant activity. IC_{50} of ABTS scavenging activity of each extract could be calculated using its calibration curve.

3. Results and Discussion

3.1 Quality of raw material

Chemical and physical properties of defatted Riceberry bran are presented in Table 1. Defatted Riceberry bran had low moisture content and aw and dark purple in color. The particle size of Riceberry bran was mostly 60-80 mesh.

Table 1. Chemical and physical properties of Riceberry bran.

Chemical and physical properties	Measurement values
Moisture (%)	5.65±0.12
a_w	0.33±0.01
L*	35.33±0.17
a*	5.69±0.11
b*	4.28±0.12
Particle size 20-40 Mesh (%)	4.55±0.78
40-60	19.24±0.95
60-80	65.16±0.86
80-100	7.80±0.84
≥ 100	3.25±0.75

3.2 Effect of extraction methods on total phenolic and total anthocyanin content

The extracts obtained from ASE, UAE, SE and MC were investigated. Percentage of extraction yield, total phenolic and total anthocyanin contents are shown in Table 2. There were no significantly differences in the percentage of extraction yield ($p>0.05$). The percentages of extraction yield from each method were in the range of 18.07–21.73%. Total phenolic content was determined in comparison with gallic acid and the results were shown in terms of mg GAE/g extract. The results showed that the Riceberry bran extract from ASE had significantly higher total phenolic and total anthocyanin content than the other methods. This method uses high pressures during the extraction process so they allow the solvent to be heated at higher temperatures than their boiling point which increases diffusion rates, disturbs the strong solute–matrix interactions and reduces liquid solvent viscosity, allowing better penetration into the matrix and then improving extraction (Barros et al., 2013). Total phenolic content of the Riceberry bran extract from SE was 54.18 mg GAE/g extract while total anthocyanin content was 0.91 mg/g extract. The increase of total phenolic content in the Riceberry bran extract from SE due to high temperature and long extraction time. During extraction, heating of the sample might soften the plant tissue and weaken the phenol–protein and phenol–polysaccharide interactions, leading to more polyphenols diffusion into the solvent (Das, Goud, & Das, 2017; Tao, Wu, Zhang, & Sun, 2014). The Riceberry bran extract from UAE has

Vol.07, No.1 DOI: 10.14456/ssstj.2020.1

Suan Sunandha Science and Technology Journal

lower total phenolic content than other methods because it took a shorter extraction time than MC and lower temperature than SE.

There were significant differences in total anthocyanin content ($p \leq 0.05$). The results obtained from four methods showed that the Riceberry bran extract from ASE had higher total anthocyanin content than the other methods because this method took a short time to heat. This result was in agreement with previous reports that ASE was more appropriate in extracting anthocyanin from colored grains as being comparable with the commonly used solvent extraction method based on changes in anthocyanin composition (Abdel-Aal et al., 2014). The Riceberry bran extract from UAE had higher anthocyanin than the Riceberry bran extract from SE and MC since ultrasound induced swelling of plant cells or breakdown of cell walls during sonication.

Table 2. Effect of extraction methods on a percentage of extract yield, total phenolic content and total anthocyanin content.

Method	Extract yield[ns] (%)	Total phenolic (mgGAE/g extract)	Total anthocyanin (mg/g extract)
ASE	20.97±0.07	55.45±0.11[a]	3.06±0.13[a]
UAE	19.57±0.11	48.52±0.50[d]	2.28±0.13[b]
SE	18.07±0.45	54.18±0.60[b]	0.91±0.07[d]
MC	21.73±0.25	50.03±0.17[c]	1.44±0.21[c]

[a-c] Means in same columns followed by different letter are significantly different ($p \leq 0.05$).

[ns] Means not significant ($p > 0.05$).

Therefore, antioxidants can be released from plant cells into the solvent. A decrease in anthocyanin of the Riceberry bran extract from SE because the extract was obtained high temperature and long extraction time as a result that anthocyanin was decomposed. An increase in temperature up to 74°C could increase phenolic content but it decreased anthocyanin content (Cacace & Mazza, 2003; Sripum, Kukreja, Charoenkiatkul, Kriengsinyos, & Suttisansanee, 2017). The degradation rate of anthocyanin depends on time and temperature. Therefore, high temperature and short extraction time were used successfully to retard anthocyanin degradation in plants (Ju & Howard, 2003).

3.3 Effect of extraction methods on radical scavenging activities

The radical scavenging activities of Riceberry bran were evaluated for DPPH, ABTS and FRAP assay as shown in Table 3. DPPH, ABTS radical scavenging activity of different extraction methods which express in terms of IC_{50} value. Lower IC_{50} value means more antioxidant potential. The chelating ability on ferrous ion in Riceberry bran extract was determined by FRAP assay. The radical scavenging activities were compared with ascorbic acid, α-tocopherol and BHT as standard. There were significantly different in IC50 of DPPH and ABTS assay and FRAP assay amongst the extraction methods ($p \leq 0.05$).

Table 3. Effect of extraction methods on radical scavenging activities (DPPH, ABTS and FRAP assay).

Method	DPPH assay IC_{50} (mg/mL)	ABTS assay IC_{50} (mg/mL)	FRAP assay mmole Fe(II)/kg
ASE	0.109±0.000[a]	3.42±0.05[a]	688.04±1.12[a]
UAE	0.144±0.004[d]	4.16±0.04[c]	543.51±0.67[c]
SE	0.127±0.000[b]	3.45±0.06[a]	649.76±0.99[b]
MC	0.137±0.002[c]	3.75±0.06[b]	668.65±1.22[ab]
BHT	0.135±0.002	0.499±0.002	3,937.00±10.00
Ascorbic acid	0.004±0.001	0.207±0.002	5,943.00±10.07
α-tocopherol	0.117±0.000	0.779±0.014	15,471.00±23.01

[a-d] Means in same columns followed by different letter are significantly different ($p \leq 0.05$).

[ns] Means not significant ($p > 0.05$).

The results showed that the Riceberry bran extract from ASE had lower IC_{50} of DPPH and ABTS assay than the other methods. The IC_{50} of DPPH assay in the Riceberry bran extract from ASE was 0.109 mg/mL which was comparatively lower than the IC_{50} of DPPH assay in BHT and α-tocopherol, the IC_{50} showed that the Riceberry bran extract from ASE had more effective antioxidant activities than antioxidant compared to BHT and α-tocopherol. Previously, Soradech et al. (2016) compared IC_{50} of six species of colored rice and it was found that the extract of Gum-Doy-Moo-Ser and Riceberry had an effective antioxidant activities than other species of colored rice in that study.

The IC_{50} of ABTS in the Riceberry extract from ASE was not significantly different from SE but significantly lower than UAE and MC ($p \leq 0.05$). The Riceberry bran extract from ASE and SE has more effective antioxidant activities than UAE and MC. The FRAP values from each method were in the range of 543.51–688.04 mmole Fe(II)/kg. The highest FRAP value was the Riceberry bran extract from ASE. There were no significant differences in FRAP value of the Riceberry bran extract from ASE and MC method ($p > 0.05$). The Riceberry bran extraction from UAE showed weak radical scavenging activities despite of high total anthocyanin content. The results indicated that

Vol.07, No.1 DOI: 10.14456/ssstj.2020.1

Suan Sunandha Science and Technology Journal

phenolic gave antioxidant activity greater than anthocyanin. This result is in agreement with the previous report by Chen, Nagao, Itani, & Irifune (2012) that anthocyanin pigments of colored rice gave a low antioxidant activities.

Table 4. The Pearson's correlation coefficient (r) between total phenolic content and antioxidant activities measured by DPPH, ABTS and FRAP assays.

	TPC	DPPH	ABTS	FRAP
TPC	1			
DPPH	-0.933*	1		
ABTS	-0.936*	0.841*	1	
FRAP	0.853*	-0.822*	-0.959*	1

* Means correlation is significant ($p \leq 0.01$).

Pearson's correlation coefficients between total phenolic content and antioxidant activities measured by DPPH, ABTS and FRAP assays were computed and the results are shown in table 4. Significant correlations were found between total phenolic content and antioxidant activity ($p \leq 0.01$) but the results of antioxidant activities were not significantly correlate to total anthocyanin content. Total phenolic content had negative correlation with IC_{50} of DPPH assay and IC_{50} of ABTS assay (r = -0.933 and r = -0.936). Significant positive correlation was obtained for total phenolic content with FRAP value (r = 0.853). The highest correlation was found between FRAP value and IC_{50} of ABTS assay (r = -0.959). The lowest correlation was found between the IC_{50} of DPPH assay and FRAP value (r = -0.822). These results corresponded to the previous research (Dudonne, Vitrac, Coutiere, Woillez, & Merillon, 2009), which reported that significant correlations were found between DPPH, ABTS, and FRAP assays and total phenolic content determined by the Folin-Ciocalteu method. Therefore, phenolic compounds in plant extracts contribute significantly to their antioxidant potential.

4. Conclusion

Analysis of the total phenolic and anthocyanin content and radical scavenging activities of Riceberry extracts showed differences depending on extraction method. Amongst the extraction methods, The Riceberry bran extraction from ASE was the most effective method in antioxidative reactions and high total phenolic and total anthocyanin content. It can be concluded that the Riceberry bran extraction SE had high total phenolic content and strong antioxidative reactions but it had a long extraction time and high costing. The Riceberry bran extract from UAE had high total anthocyanin content and it used the lower energy input. The Riceberry bran extract from MC had low bioactive compounds and antioxidant activities but it took a long extraction time.

5. Acknowledgement

This research was supported by department of product development, faculty of agro-industry, Kasetsart university and Kasetsart agicultural and agro-industrial product improvement institute.

6. Publication Ethic

Submitted manuscripts must not have been previously published by or be under review by another print or online journal or source.

7. References

Abdel-Aal, E., Akhtar, H., Rabalski, I., & Bryan, M. (2014). Accelerated, microwave-assisted, and conventional solvent extraction methods affect anthocyanin composition from colored grains. *Journal of Food Science*, *79*(2), C138-C146.

Association of Official Analytical Chemists. (2019). *Official methods of analysis* (21st ed.). Washington DC: Author.

Barros, F., Dykes, L., Awika, J. M., & Rooney, L. W. (2013). Accelerated solvent extraction of phenolic compounds from sorghum brans. *Journal of Cereal Science*, *58*(2), 305-312.

Benzie, I. F. F., & Strain, J. J. (1999). Ferric reducing/antioxidant power assay: Direct measure of total antioxidant activity of biological fluids and modified version for simultaneous measurement of total antioxidant power and ascorbic acid concentration. *Methods in Enzymology*, 299, 15-27.

Cacace, J. E., & Mazza, G. (2003). Optimization of extraction of anthocyanins from black currants with aqueous ethanol. *Journal of Food Science*, *68*(1), 240-248.

Chen, X. Q., Nagao, N., Itani, T., & Irifune, K. (2012). Anti-oxidative analysis, and identification and quantification of anthocyanin pigments in different coloured rice. *Food Chemistry*, *135*(4), 2783-2788.

Das, A. B., Goud, V. V., & Das, C. (2017). Extraction of phenolic compounds and anthocyanin from black and purple rice bran (*Oryza sativa* L.) using ultrasound: A comparative analysis and phytochemical profiling. *Industrial Crops and Products*, *95*, 332-341.

Suan Sunandha Science and Technology Journal

Dudonne, S., Vitrac, X., Coutiere, P., Woillez, M., & Merillon, J. (2009). Comparative study of antioxidant properties and total phenolic content of 30 plant extracts of industrial interest using DPPH, ABTS, FRAP, SOD, and ORAC assays. *Journal of Agricultural and Food Chemistry*,*57*(5),1768-1774

Giusti, M. M., & Wrolstad, R. E. (2005). Characterization and measurement of anthocyanins by UV-visible spectroscopy. *Current Protocols in Food Analytical Chemistry*, *1*, F1.2.1-F1.2.13.

Ju, Z. Y., & Howard, L. R. (2003). Effects of solvent and temperature on pressurized liquid extraction of anthocyanins and total phenolics from dried red grape skin. *Journal of Agricultural and Food Chemistry*, *5*1, 5207-5213.

Leardkamolkarn, V., Thongthep, W., Suttiarporn, P., Kongkachuichai, R., Wongpornchai, S., & Wanavijitr, A. (2011). Chemopreventive properties of the bran extracted from a newly developed Thai rice: The Riceberry. *Food Chemistry*, *125*(3), 978-985. doi:10.1016/j.foodchem.2010.09.093

Peanparkdee, M., Yamauchi, R., & Iwamoto, S. (2018). Characterization of antioxidants extracted from Thai Riceberry bran using ultrasonic-assisted and conventional solvent extraction methods. *Food and Bioprocess Technology*, *11*, 713-722.

Posuwan, J., Prangthip, P., Leardkamolkarn, V., Yamborisut, U., Surasiang, R., Charoensiri, R., & Kongkachuichai, R. (2013). Long-term supplementation of high pigmented rice bran oil (*Oryza sativa* L.) on amelioration of oxidative stress and histological changes in streptozotocin-induced diabetic rats fed a high fat diet; Riceberry bran oil. *Food Chemistry*, *138*(1), 501-508.

Prangthip, P., Surasiang, R., Charoensiri, R., Leardkamolkarn, V., Komindr, S., Yamborisut, U. … Kongkachuichai, R. (2013). Amelioration of hyperglycemia, hyperlipidemia, oxidative stress and inflammation in steptozotocin-induced diabetic rats fed a high fat diet by Riceberry supplement. *Journal of Functional Foods*, *5*, 195-203.

Re, R., Pellegrini, N., Proteggente, A., Pannala, A., Yang, M., & Rice-Evans, C. (1999). Antioxidant activity applying an improved ABTS radical cation decolorization assay. *Free Radical Biology and Medicine*, *26* (9-10), 1231-1237.

Soradech, S., Reungpatthanaphong, P., Tangsatirapakdee, S., Panaphong, K., Thammachat, T., Manchun, S., & Thubthimthed, S. (2016). Radical scavenging, antioxidant and melanogenesis stimulating activities of different species of rice (*Oryza sativa* L.) extracts for hair treatment formulation. *Thai Journal of Pharmaceutical Science*, *40*, 92-95.

Sripum, C., Kukreja, R. K., Charoenkiatkul, S., Kriengsinyos, W., & Suttisansanee, U. (2017). The effect of extraction conditions on antioxidant activities and total phenolic contents of different processed Thai Jasmine rice. *International Food Research Journal*, *24*(4), 1644-1650.

Suttiarporn, P., Sookwong, P., & Mahatheeranont, S. (2016). Fractionation and identification of antioxidant compounds from bran of Thai Black Rice cv. Riceberry. *International Journal of Chemical Engineering and Applications*, *7*(2), 109-114.

Tabaraki, R., & Nateghi, A. (2011). Optimization of ultrasonic-assisted extraction of natural antioxidants from rice bran using response surface methodology. *Ultrasonics Sonochemistry*, *18*(6), 1279-1286.

Tao, Y., Wu, D., Zhang, Q., & Sun, D. (2014). Ultrasound-assisted extraction of phenolics from wine lees: Modeling, optimization and stability of extracts during storage. *Ultrasonics Sonochemistry*, *21*(2), 706-715.

Wolfe, K., Wu, X., & Liu, R. H. (2003). Antioxidant activity of apple peels. *Journal of Agricultural and Food Chemistry*, *51*, 609-614.

Available online at http://www.ssstj.sci.ssru.ac.th

Suan Sunandha Science and Technology Journal

DFT Investigation of Toluene Adsorption on Silicon Carbide Nanosheet Doping with Transition Metal for Storage and Sensor Application

Pasakorn Sangnikul[1*], Chanukorn Tabtimsai[1,], Wandee Rakrai[1], Banchob Wanno[2]**

[1] Computational Chemistry Center for Nanotechnology and Department of Chemistry, Faculty of Science and Technology, Rajabhat Maha Sarakham University, Maha Sarakham 44000, Thailand

[2] Center of Excellence for Innovation in Chemistry and Supramolecular Chemistry Research Unit, Department of Chemistry, Faculty of Science, Mahasarakham University, Maha Sarakham 44150, Thailand

Corresponding author e-mail: *champ9yod@gmail.com,tabtimsai.c@gmail.com**

Received: *6 January 2020* / **Revised:** *20 January 2020* / **Accepted:** *30 January 2020*

Abstract

Nowadays, the emission of volatile organic compounds (VOC) is giving rise to several health hazards and damage to the environment. Consequently, the nanomaterial development is considerably important for VOC adsorption and sensing. In this work, the adsorptions of toluene on silicon carbide nanosheets doping with transition metal atoms (TM-doped SiCNS) were investigated using the density functional theory method (DFT). The B3LYP/LanL2DZ was employed in all calculations for the geometric, energetic, and electronic properties. In addition, the doping of TM atom at different sites will have different effects on the adsorption behavior of the systems. Calculation results reveal that the adsorption distances and adsorption energies of TM doping on SiCNSs are suitable for toluene adsorption greater than pristine SiCNS. According to the changes of electronic properties of TM-doped SiCNS show highly sensitive to toluene molecule. The results indicate that the introducing of TM doping on SiCNS significantly improve the sensitivity toward toluene molecule. Therefore, the results of our work may be useful in developing and designing new types of storage and sensor materials.

Keywords: DFT, Silicon carbide nanosheet, Toluene, Transition metals, VOC

1. Introduction

Volatile organic compounds (VOC) are common air pollutants emitted by the chemical industries such as production of adhesives, paints, printing materials, building materials, and chemicals for synthesis (Kim et al., 2019). For this reason, it is an important issue to develop sensors for detect and manage VOC. In the recent year, the experimental and theoretical studies about VOC adsorption on different nanostructures have been reported widely (Chiang et al., 2001; Su et al., 2018). Manaschai Kunaseth et al. have investigated the adsorption of VOC on transition metal deposited graphene which adsorption energy of benzene was -1.93 eV calculated by using Perdew-Wang functional (PW91) (Kunaseth et al., 2017). The para-nitrophenol molecule adsorption on vacancy and Pt-doped graphene sheets showed that the adsorption capacity of graphene can be significantly increased (Mandeep et al., 2018). Toluene is volatile organic compound that evaporate at room temperature. Toluene is harmful to human health, and may cause various diseases such as headache, nausea, coryza, pharyngitis, emphysema, lung cancer, and even death (Yi et al., 2008). Also study of the adsorptions of VOCs on activated carbon/metal oxide composites have been performed by Ke Zhou et al, that calculation shows that the highest adsorption energy of toluene on activated carbon was -20.87 kJ/mol calculated by using JW-BK132Z functional (Zhou et al., 2019). Lian Yu et al. have reported the adsorption of VOC on reduced graphene oxide, and the results suggested that graphene oxide is excellent adsorption performance for toluene molecule (Yu et al., 2018). As previously mentioned, Experimental and theoretical studies on the adsorption of VOC are showed extremely interesting and it is necessary to understand more.

The silicon carbide nanosheet (SiCNS) has recently attracted considerable attention due to it has the notable properties such as thermal stability, chemical inertness, high thermal conductivity, and others (Delavari & Jafari., 2018; Ansari et al., 2013).

Suan Sunandha Science and Technology Journal

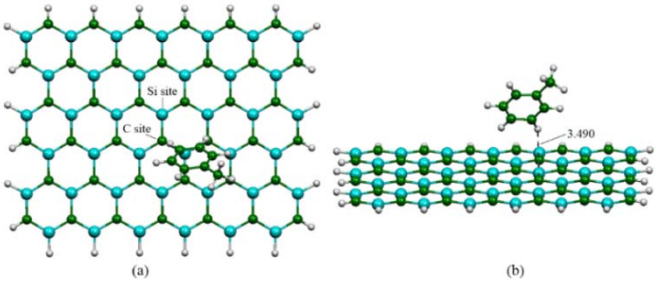

Figure 1. The B3LYP/LanL2DZ optimized structures of top views of (a) pristine SiCNS and (b) toluene adsorbed on pristine SiCNS

They also have wide range of applications in different fields such as energy conversion, enhance materials strength, gas storage and sensing applications (Chabi et al., 2016). However, pristine SiCNS has been explored as low efficient for adsorption or storage and low sensitive to small molecule (Wang et al., 2016). Therefore, many studies are devoted to improving the surface sensibility of silicon carbide nanostructures by introducing doping metal atoms. Doping of transition metal (TM=Fe, Co, Al, Cu, and Zn) atoms on SiCNS can improve the adsorption abilities of TM-doped SiCNS to small molecule and change electronic properties of TM-doped SiCNS (Sun et al., 2016). Ga- and B-doped SiCNSs show better capability of small molecule adsorption capability than undoped SiCNS (Tabtimsai et al., 2015). The silicon carbide nanotube (SiCNT) doping with group 8B transition metal are appropriate for hydrogen storage and show better hydrogen adsorption capability than undoped SiCNT (Tabtimsai et al., 2018).

To the best of our knowledge, there are no reports the adsorption abilities of toluene molecule on TM-doped SiCNS. Therefore, aim of this work, we investigate the geometric, energetic, and electronic properties of pristine and TM-doped SiCNSs by density functional theory (DFT) and subsequently we evaluate their ability in adsorption of toluene molecules.

2. Computational details

The structure optimization of SiCNS ($C_{39}Si_{39}H_{24}$) was modeled and used. The edges of the sheet were saturated by hydrogen atoms to avoid the boundary effects. The doping of TM atom on the center of SiCNS was modeled. The transition metal atoms, i.e., V, Nb, Ta, Cr, Mo, W, Mn, Tc, and Re were doping on carbon (TM_C) or silicon (TM_{Si}) atom at the center of SiCNS. Therefore, systems of TM-doped on SiCNS were considered the spin-polarized restricted and unrestricted optimizations. Geometrical optimizations of their systems were taken under the DFT calculation. The calculation was performed under hybrid density functional B3LYP, Becke's three parameter exchange functional with the Lee-Yang-Parr correlation functional (B3LYP) (Becke., 1988, 1993; Lee., 1988) and the Los Alamos LanL2DZ split-valence basis set (Hay & Wadt., 1985a, 1985b; Wadt & Hay., 1985). All calculations were performed by using GAUSSIAN 09 program (Frisch et al., 2009). The geometrical parameters as equilibrium structural and natural bond orbitals (NBO) charges of studied compounds were specified at T= 0 K. The molecular graphics of all related species were generated with the MOLEKEL 4.3 program (Flükiger et al., 2000). The electronic density of states (DOSs) of all systems were plotted by the GaussSum 2.2 program (O'boyle et al., 2008). Adsorption energy (E_{ads}) of toluene

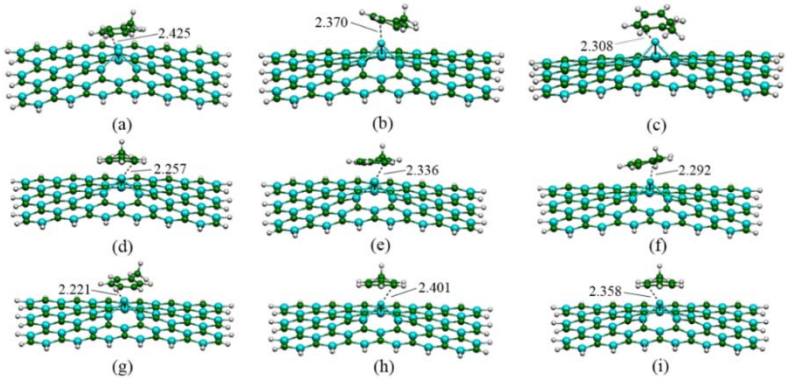

Figure 2. The B3LYP/LanL2DZ optimized structures of toluene adsorbed on TM_C-SiCNSs, (a) toluene/V_C-, (b) toluene/Nb_C-, (c) toluene/Ta_C-, (d) toluene/Cr_C-, (e) toluene/Mo_C-, (f) toluene/W_C-, (g) toluene/Mn_C-, (h) toluene/Tc_C-, and (i) toluene/Re_C-doped SiCNSs.

Vol.07, No.1 DOI: 10.14456/ssstj.2020.3

Suan Sunandha Science and Technology Journal

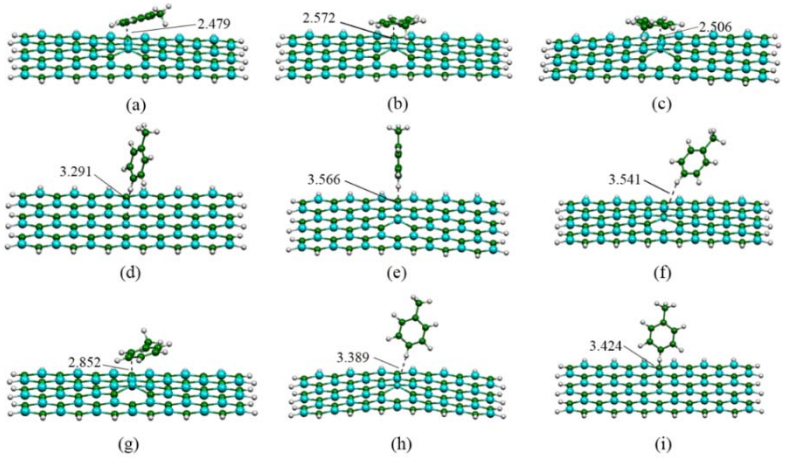

Figure 3. The B3LYP/LanL2DZ optimized structures of toluene adsorbed on TM_{Si}-SiCNSs (a) toluene/V_{Si}-,(b) toluene/Nb_{Si}-, (c) toluene/Ta_{Si}-, (d) toluene/Cr_{Si}- (e) toluene/Mo_{Si}- (f) toluene/W_{Si}- (g) toluene/Mn_{Si}- (h) toluene/Tc_{Si}-, and (i) toluene/Re_{Si}-doped SiCNSs.

molecule adsorbed on the pristine and TM-doped SiCNS were obtained from equations

$$E_{ads} = E_{toluene/SiCNS\ or\ TM\text{-}SiCNS} - (E_{SiCNS\ or\ TM\text{-}SiCNS} + E_{toluene}) \quad (1)$$

, where $E_{toluene/SiCNS\ or\ TM\text{-}SiCNS}$ are the total energy of the adsorption of toluene molecule on pristine or TM-doped SiCNS. The $E_{SiCNS\ or\ TM\text{-}SiCNS}$ and $E_{toluene}$ are the total energies of pristine or TM-doped SiCNS and toluene molecule, respectively. Considering the electronic properties in term of the highest occupied molecular orbital energies (E_{HOMO}), the lowest unoccupied molecular orbital energies (E_{LUMO}), the energy gaps (E_{gap}) referred to the energy difference between HOMO and LUMO orbitals and changes of energy gaps (ΔE_{gap}) referred to the gap difference between before and after gas adsorption were investigated at the same theoretical level.

3. Results and discussion

3.1 Geometrical structures

The B3LYP/LanL2DZ-optimized structures of the pristine and their adsorption with toluene molecule are displayed in Figure 1. In addition, the doping sites are showed in Figure 1a. The calculated average Si-C bond lengths and bond angles of pristine SiCNS are found to be 1.780 Å and 120.0º, respectively, which are in accordance with the previous reports (Delavari & Jafari., 2018). The bond lengths, bond angles, and adsorption distances of toluene adsorbed on pristine, V-, Nb-, Ta-, Cr-, Mo-, W-, Mn-, Tc-, and Re-doped SiCNSs are listed in Table 1. In comparison of pristine SiCNS with the toluene adsorbed on pristine SiCNS (toluene/SiCNS), the bond lengths and bond angles of pristine SiCNS system are slightly changed. Therefore, toluene/SiCNS reflected that toluene molecule occur the weak interaction.

The toluene adsorptions on TM_C-SiCNS (toluene/TM_C-SiCNS) are showed in Figure 2., the Si-TM bond lengths are in the ranges of 2.294-2.563 Å, while the Si-TM-Si bond angles are in the ranges of 78.6-97.3º. Obviously, after toluene adsorption, the surface of TM_C-SiCNS still reveal the protruded geometrical structures which were similar trends can be found in other works (Farmanzadeh & Ardehjani., 2018). In another hand, the

B3LYP/LanL2DZ-optimized structures of toluene/TM_{Si}-SiCNS are displayed in Figure 3. The C-TM bond lengths of toluene/TM_{Si}-SiCNS obtained in this study are in the ranges of 1.825 - 2.035 Å, which are significantly shorter than C-TM of TM_C-SiCNS, while the bond angles of C-TM-C at the doping site of toluene/TM_{Si}SiCNS$_{Si}$ are in the range of 107.5 - 121.0º, which were wider than that of the Si-TM-Si bond angles of toluene/TM_C-SiCNS.

The adsorption distances (AD) between toluene molecule and pristine SiCNS or TM-doped SiCNS are listed in Table 1. The AD between toluene molecule and the pristine SiCNS is calculated to be 3.490 Å. The AD between the toluene molecule and TM-SiCNSs are found in the range 2.234-2.476 and 2.479-3.566 Å for TM_C-SiCNS and TM_{Si}-SiCNS, respectively. This indicates that interactions between toluene molecule and TM_C-SiCNS are stronger than TM_{Si}-SiCNS.

Vol.07, No.1 DOI: 10.14456/ssstj.2020.3

Suan Sunandha Science and Technology Journal

Table 1. The selected geometrical parameters and adsorption distances (AD) of toluene molecule adsorbed on pristine and TM-doped SiCNS.

Species	Si1-TM or C1-TM (Å)	Si2-TM or C2-TM (Å)	Si3-TM or C3-TM (Å)	Si1-TM-Si2 or C1-TM-C2 (º)	Si1-TM-Si3 or C1-TM-C3 (º)	Si2-TM-Si3 or C2-TM-C3 (º)	AD (Å)
toluene/SiCNS	1.798 [a]	1.824 [a]	1.798 [a]	119.3[a]	121.2[a]	119.3[a]	3.490
toluene/V_C-SiCNS	2.464	2.481	2.465	83.3	86.1	83.4	2.476
toluene/Nb_C-SiCNS	2.513	2.546	2.510	84.3	85.0	78.5	2.370
toluene/Ta_C-SiCNS	2.554	2.534	2.546	82.4	81.4	83.1	2.309
toluene/Cr_C-SiCNS	2.415	2.315	2.311	80.9	85.0	96.4	2.234
toluene/Mo_C-SiCNS	2.398	2.563	2.393	80.6	94.5	79.9	2.336
toluene/W_C-SiCNS	2.437	2.479	2.426	81.5	88.6	86.4	2.292
toluene/Mn_C-SiCNS	2.294	2.310	2.320	91.0	87.9	86.7	2.267
toluene/Tc_C-SiCNS	2.355	2.427	2.353	85.2	92.0	85.2	2.473
toluene/Re_C-SiCNS	2.368	2.427	2.368	85.5	91.4	85.5	2.358
toluene/V_{Si}-SiCNS	1.891	1.983	1.884	109.2	115.2	109.6	2.479
toluene/Nb_{Si}-SiCNS	1.986	2.035	1.982	107.6	108.3	107.5	2.572
toluene/Ta_{Si}-SiCNS	1.978	2.023	1.982	107.5	108.5	107.6	2.506
toluene/Cr_{Si}-SiCNS	1.825	1.883	1.825	119.4	121.0	119.4	3.291
toluene/Mo_{Si}-SiCNS	1.932	1.982	1.930	113.2	114.5	113.1	3.566
toluene/W_{Si}-SiCNS	1.933	1.964	1.933	116.9	116.9	116.9	3.541
toluene/Mn_{Si}-SiCNS	1.938	1.972	1.938	109.2	112.5	109.4	2.852
toluene/Tc_{Si}-SiCNS	1.938	1.972	1.938	110.2	111.2	110.3	3.389
toluene/Re_{Si}-SiCNS	1.880	1.914	1.880	120.3	119.3	120.3	3.424

[a] Bond lengths and bond angles of toluene adsorbed on pristine SiCNS

3.2 Adsorption abilities of pristine and TM-doped SiCNSs onto toluene adsorbed

The adsorption energies (E_{ads}) of toluene adsorbed on the pristine, V-, Nb-, Ta-, Cr-, Mo-, W-, Mn-, Tc-, and Re-doped SiCNSs are listed in Table 2. The adsorption energy of toluene adsorbed on pristine SiCNS is -0.416 kcal/mol. This confirms that pristine SiCNS is slightly sensitive to toluene molecule. The adsorption energies of toluene adsorbed on TM_C-doped SiCNS are in a range of -51.604 and -30.922 kcal/mol. Their E_{ads} are in the following order: toluene/W_C-SiCNS (-51.604 kcal/mol) > toluene/Cr_C-SiCNS (-46.172 kcal/mol) > toluene/Mo_C-SiCNS (-41.204 kcal/mol) > toluene/Ta_C-SiCNS (-40.483 kcal/mol) > toluene/Mn_C-SiCNS (-38.511 kcal/mol) > toluene/Re_C-SiCNS (-35.833 kcal/mol) ≈ toluene/V_C-SiCNS (-35.583 kcal/mol) ≈ toluene/Nb_C-SiCNS (-35.469 kcal/mol) > toluene/Tc_C-SiCNS (-30.922 kcal/mol). The parameters of adsorption energies indicate that the TM_C-SiCNS are exothermic reactions. Surprisingly, the TM doping on C site significantly improved adsorption ability of SiCNS. The large adsorption energies and short AD reflected that toluene molecule underwent the strong interaction with TM_C-doped SiCNS. These adsorption energies were in according to concordance with the previous studies (Su et al., 2018).

The adsorption energies of toluene adsorbed on TM_{Si}-doped SiCNS are also exothermic reactions which are in the range of -34.004 to -0.027 kcal/mol. Their E_{ads} order is found as follow: toluene/Mn_{Si}-SiCNS (-34.004 kcal/mol) > toluene/Ta_{Si}-SiCNS (-14.721 kcal/mol) ≈ toluene/Nb_{Si}-SiCNS (-13.747 kcal/mol) > toluene/V_{Si}-SiCNS (-5.815 kcal/mol) > toluene/Re_{Si}-SiCNS (-1.060 kcal/mol) ≈ toluene/Cr_{Si}-SiCNS (-1.021 kcal/mol) ≈ toluene/W_{Si}-SiCNS (-0.997 kcal/mol) > toluene/Mo_{Si}-SiCNS (-0.027 kcal/mol). The TM doping on Si site also improved adsorption ability of SiCNS. Therefore, the Mn_{Si}-SiCNS, Ta_{Si}-SiCNS, Nb_{Si}-SiCNS and V_{Si}-SiCNS are suitable adsorption energies and short AD that toluene molecule underwent the strong interaction with TM_{Si}-doped SiCNS. Except for the Re_{Si}-SiCNS, Cr_{Si}-SiCNS, W_{Si}-SiCNS, Mo_{Si}-SiCNS, and Tc_{Si}-SiCNS display the small adsorption energies, and large AD reflected that toluene molecule underwent the weak

Vol.07, No.1 DOI: 10.14456/ssstj.2020.3

Suan Sunandha Science and Technology Journal

Table 2. Adsorption energies (E_{ads}), E_{HOMO}, E_{LUMO}, E_{gap}, ΔE_{gap}, and partial charge transfers (PCT) of toluene molecule adsorbed on pristine and TM-doped SiCNSs, computed at the B3LYP/LanL2DZ level of theory.

Species	E_{ads} (kcal/mol)	E_{HOMO} (eV)	E_{LUMO} (eV)	E_{gap} (eV)	ΔE_{gap} (eV)	PCT (e)
toluene/SiCNS	-0.416	-3.919	-3.728	0.190	0.027	0.007
toluene/V_C-SiCNS	-35.583	-4.027	-3.293	0.735	-0.408	0.341
toluene/Nb_C-SiCNS	-35.469	-3.973	-3.728	0.245	0.218	0.162
toluene/Ta_C-SiCNS	-40.483	-4.055	-3.565	0.490	-0.245	0.052
toluene/Cr_C-SiCNS	-46.172	-3.837	-3.646	0.190	0.000	0.448
toluene/Mo_C-SiCNS	-41.204	-3.837	-3.619	0.218	-0.082	0.437
toluene/W_C-SiCNS	-51.604	-3.864	-3.646	0.218	0.109	0.303
toluene/Mn_C-SiCNS	-38.511	-4.082	-3.265	0.816	-0.082	0.414
toluene/Tc_C-SiCNS	-30.922	-4.055	-3.456	0.599	-0.109	0.283
toluene/Re_C-SiCNS	-35.833	-3.837	-3.646	0.190	0.000	0.204
toluene/V_{Si}-SiCNS	-5.815	-4.055	-3.374	0.680	0.163	0.204
toluene/Nb_{Si}-SiCNS	-13.747	-3.782	-3.402	0.381	0.463	0.212
toluene/Ta_{Si}-SiCNS	-14.721	-3.755	-3.402	0.354	0.490	0.236
toluene/Cr_{Si}-SiCNS	-1.021	-3.973	-3.755	0.218	0.000	-0.092
toluene/Mo_{Si}-SiCNS	-0.708	-3.973	-3.755	0.218	-0.027	-0.002
toluene/W_{Si}-SiCNS	-0.997	-3.973	-3.755	0.218	0.000	-0.002
toluene/Mn_{Si}-SiCNS	-34.004	-4.163	-3.347	0.816	-0.027	0.155
toluene/Tc_{Si}-SiCNS	7.531	-4.163	-3.402	0.762	0.163	0.003
toluene/Re_{Si}-SiCNS	-1.060	-3.919	-3.538	0.381	0.136	0.001

interaction. Whereas, the toluene adsorbed on Tc_{Si}-SiCNS (7.531 kcal/mol) is the endothermic reaction. Apparently, the adsorption ability of SiCNS onto toluene molecule is improved by TM doping which is similar with that of adsorption of volatile organic compounds onto Al-doped C_2N monolayer (19), and volatile organic compounds adsorption on transition metal deposited graphene (Chiang et al., 2001). Additionally, TM doping on C site of SiCNS displays higher interaction with toluene molecule than Si site. The results that are similar to previous work in which we found that Ni-doped silicon carbide nanocage displayed the higher adsorption energies of hydrogen than Si site (Goudarziafshar et al., 2018) Its cloud be concluded here that the TM doping SiCNS are much more suitable for toluene adsorption than pristine SiCNS.

3.3 Electronic properties for the systems

To further investigate the adsorption phenomenon of the toluene molecule on the pristine and TM-doped SiCNSs is investigated, then we consider the E_{HOMO}, E_{LUMO}, E_{gap}, and ΔE_{gap} of the stable configuration of toluene molecule absorbed on pristine and TM-doped SiCNSs. In Table 2, theoretical calculation reveals that the E_{gap} of toluene/SiCNS is 0.190 eV. The E_{gap} of toluene/TM_C- and TM_{Si}-SiCNSs are in the range of 0.816 to 0.190 and 0.762 to 0.218 eV, respectively, which are smaller than the E_{gap} of pristine SiCNS (E_{gap} = 2.49 eV). For the pristine SiCNS, V_C-SiCNS, Nb_C-SiCNS, Ta_C-SiCNS, Mo_C-SiCNS, W_C-SiCNS, Mn_C-SiCNS, Tc_C-SiCNS, V_{Si}-SiCNS, Nb_{Si}-SiCNS, Ta_{Si}-SiCNS, Mo_{Si}-SiCNS, Mn_{Si}-SiCNS, Tc_{Si}-SiCNS, and Re_{Si}-SiCNS systems, the E_{gap} are changed by toluene adsorption, meaning the electronic properties of the systems are also exponentially changed. The reducing of E_{gap} of TM-doped SiCNS due to toluene adsorption is in excellent agreement with the previous calculated results of TM-doped SiCNS (Farmanzadeh & Ardehjani., 2018). Except for toluene adsorption on Cr_C-SiCNS, Re_C-SiCNS, Cr_{Si}-SiCNS, and W_{Si}-SiCNS, the E_{gap} are not change.

The partial charge transfers (PCT) between toluene molecule and SiCNS were calculated. The loss and gain of electrons could also be determine

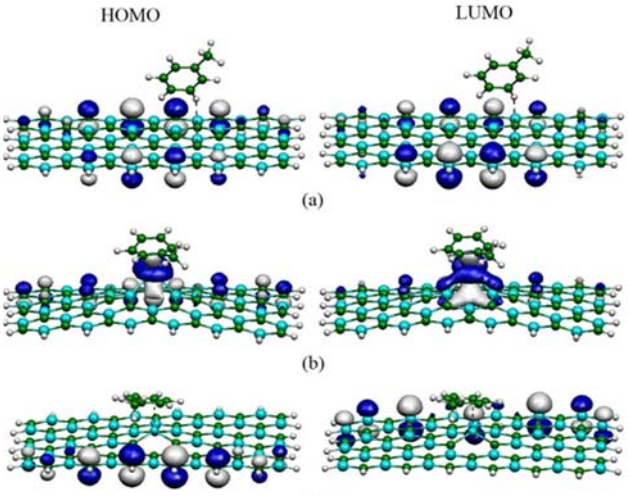

Figure 4. Plots of HOMO and LUMO distributions of (a) toluene/SiCNS, (b) toluene/TaC-SiCNS, and (c) toluene/TaSi-SiCNS.

Vol.07, No.1 DOI: 10.14456/ssstj.2020.3

Suan Sunandha Science and Technology Journal

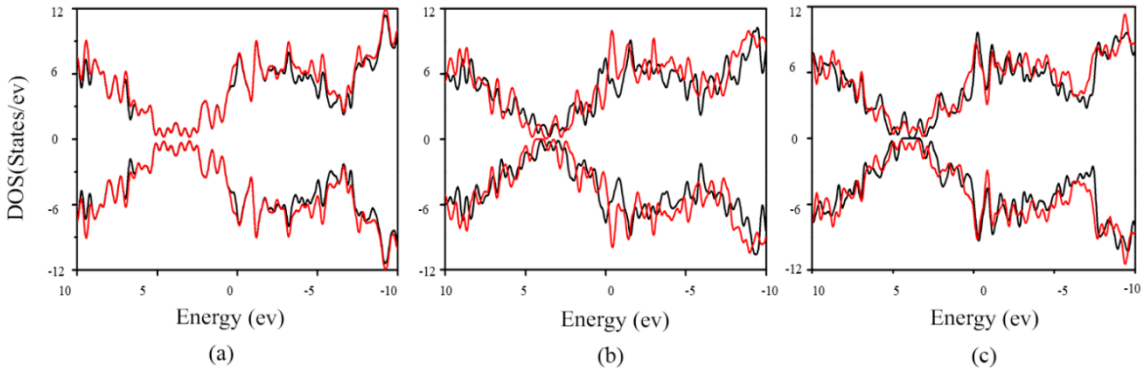

Figure 5. DOSs of (a) pristine SiCNS and toluene/SiCNS, (b) Ta_C-SiCNS and toluene/Ta_C-SiCNS, and (c) Ta_{Si}-SiCNS and toluene/Ta_{Si}-SiCNS. Before and after toluene adsorption are black and red lines, respectively.

by natural bond orbital (NBO) charge calculations before and after toluene adsorptions (Table 3). The PCT was defined as $Q_{toluene/SiCNS}$ - $Q_{toluene}$, where $Q_{touene/SiCNS}$ is the total charge of toluene adsorbed on pristine and TM-doped SiCNS, and $Q_{toluene}$ is the charge of toluene in free case. We found that the PCTs between toluene molecule and pristine SiCNS is about -0.007 e. The PCTs between toluene molecule and TM_C-SiCNS are in the ranges of 0.052 - 0.448 e. While the PCTs between toluene molecule and Mn_{Si}-SiCNS, Ta_{Si}-SiCNS, Nb_{Si}-SiCNS and V_{Si}-SiCNS are in the ranges of 0.236 - 0.155 e corresponding with strong adsorption abilities. The PCTs indicate that the large charge transfers between toluene molecule and TM_C-SiCNS and Mn_{Si}-SiCNS, Ta_{Si}-SiCNS, Nb_{Si}-SiCNS and V_{Si}-SiCNS are strongly bond due to covalent interaction. The covalent interaction between toluene molecule and TM-doped SiCNS is strong hybridization between the C's *p* orbital or H's *s* orbital of toluene and TM *d* orbital of TM-doped SiCNS. For the PCTs of toluene/TM_{Si}-SiCNS system, the PCTs between toluene molecule and Re_{Si}-SiCNS, Cr_{Si}-SiCNS, W_{Si}-SiCNS, Mo_{Si}-SiCNS, and Tc_{Si}-SiCNS are in the ranges of 0.001 to -0.092 e corresponding with weak adsorption abilities. Therefore, computations demonstrate that weak adsorption abilities of pristine SiCNS, Re_{Si}-SiCNS, Cr_{Si}-SiCNS, W_{Si}-SiCNS, Mo_{Si}-SiCNS, and Tc_{Si}-SiCNS slightly sensitive to toluene molecule.

Moreover, the HOMO and LUMO orbital distributions of the toluene adsorptions on pristine and TM-doped SiCNSs are also reported. The results show that, for toluene/SiCNS and toluene/TM_{Si}-SiCNS systems, the HOMO and LUMO orbitals are localized around the sheet (Figures. 4a and 4c.). Whereas, the HOMO and LUMO orbitals of TM_C-SiCNS are localized on the adsorption sites. The localization of the HOMO and LUMO orbitals of the toluene/Ta_C-SiCNS is clearly clustered (Figure 4b.). These results indicating the electron conduction through these systems.

The density of states were (DOSs) also calculated and plotted. The DOSs of pristine and TM-doped SiCNSs before and after toluene adsorption are displayed in Figure 5. The DOSs of pristine SiCNS are slightly changed by toluene adsorption. This confirms that toluene molecule has slightly sensible effect on the electronic properties of the pristine SiCNS (Figure 5a.). However, the DOSs of TM-doped SiCNS such as Ta_C-and Ta_{Si}-doped SiCNSs are significantly changed by toluene adsorption. These results are similar with Fe-doped SiCNS, reported by D. Farmanzadeh & Ardehjani (Farmanzadeh & Ardehjani., 2018). The changes of the DOSs are expected to bring about obvious changes in the corresponding electronic properties.

In summary, the adsorptions abilities of TM-doped SiCNS to toluene molecule are larger than that of the pristine SiCNS. This supported the notion that the TM doping has an influence on the electronic properties of the SiCNS substantially, which was consistent with the previous results of Pd-doped SiCNS(Bezi Javan et al., 2016). The results indicated that the changes of electronic properties are beneficial for sensing applications.

4. Conclusions

In order to search for novel nanomaterials for toluene storage and sensing applications, the transition metals (TM = V, Nb, Ta, Cr, Mo, W, Mn, Tc, and Re) doping on SiCNS are selected. The geometric, energetic, and electronic properties of toluene adsorption on TM-doped SiCNS are calculated using the density functional theory method at B3LYP/LanL2DZ level of theory. It is found toluene molecule displays weak adsorption on the surface of pristine SiCNS (E_{ads} = -0.416 kcal/mol), whereas toluene molecule shows strong adsorption on the surface of TM-doped SiCNSs. The W_C-doped SiCNS displays the strongest interaction

Vol.07, No.1 DOI: 10.14456/ssstj.2020.3

Suan Sunandha Science and Technology Journal

with toluene molecule (E_{ads} = -51.604 kcal/mol). The ΔE_{gap} and DOSs of the TM-SiCNSs present dramatic changes after adsorption with toluene molecules. A better understanding of these interactions is achieved by NBO analysis which confirms considerable charge transfers during the adsorption of toluene molecule onto the TM-doped SiCNS. The observations show that TM-doped SiCNSs are highly sensitive toluene molecules. Thus, TM-doped

5. Acknowledgement

The authors gratefully acknowledge the Computational Chemistry Center for Nanotechnology (CCCN) and Department of Chemistry, Faculty of Science and Technology, and Research and Development Institute, Rajabhat Maha Sarakham University for the facilities provided. Our also extends to gratitude Promotion of Science and Mathematics Talented Teachers (PSMT) for partial financial support.

6. Publication Ethic

Submitted manuscripts must not have been previously published by or be under review by another print or online journal or source.

7. References

Ansari, R., Rouhi, S., Mirnezhad, M., & Aryayi, M. (2013). Stability characteristics of single-layered silicon carbide nanosheets under uniaxial compression. Physica E: *Low-Dimensional Systems and Nanostructures*, 53, 22-28. doi:10.1016/j.physe.2013.04.014

Becke, A.D., Density-functional exchange-energy approximation with correct asymptotic behavior, *Phys. Rev*. A 38 (1988) 3098-3100.

Becke, A.D., Density-functional thermochemistry. III. The role of exact exchange, *J. Chem. Phys. 98* (1993) 5648-5652.

Bezi Javan, M., Houshang Shirdel-Havar, A., Soltani, A., & Pourarian, F. (2016). Adsorption and dissociation of H_2 on Pd doped graphene-like SiC sheet. *International Journal of Hydrogen Energy*, *41*(48), 22886-22898. doi:10.1016/j.ijhydene.2016.09.081

Chabi, S., Chang, H., Xia, Y., & Zhu, Y. (2016). From graphene to silicon carbide: ultrathin silicon carbide flakes. *Nanotechnology*, 27(7), 075602.doi:10.1088/0957-4484/27/7/075602

Chiang, Y.-C., Chiang, P.-C., & Huang, C.-P. (2001). Effects of pore structure and temperature on VOC adsorption on activated carbon. Carbon, 39(4), 523-534.

Delavari, N., & Jafari, M. (2018). Electronic and optical properties of hydrogenated silicon carbide nanosheets: A DFT study. *Solid State Communications*, 275, 1-7. doi: 10.1016/j.ssc.2018.03.004

Farmanzadeh, D., & Ardehjani, N. A. (2018). Adsorption of O_3, SO_2 and NO_2 molecules on the surface of pure and Fe-doped silicon carbide nanosheets: *A computational study. Applied Surface Science*, 462, 685-692. doi: 10.1016/j.apsusc.2018.08.150

Flükiger P., Lüthi, H.P., & Portmann, S., MOLEKEL 4.3, Swiss center for scientific computing. Manno, Switzerland, 2000.

Frisch, M.J., Trucks G.W., Schlegel H.B., Scuseria G.E., Robb M.A., Cheeseman J.R., ..., Pople J.A. GAUSSIAN 09, Revision A.02, Gaussian Inc, WallingfordCT, 2009.

Goudarziafshar, H., Abdolmaleki, M., Moosavi-zare, A. R., & Soleymanabadi, H. (2018). Hydrogen storage by Ni-doped silicon carbide nanocage: *A theoretical study. Physica E: Low-Dimensional Systems and Nanostructures*, 101, 78-84.doi: 10.1016/j.physe.2018.03.001

Hay P.J., Wadt W.R., Ab initio effective core potentials for molecular calculations. Potentials for K to Au including the outermost core orbitals. *J. Chem. Phys*. 82(1985) 299-310.

Hay, P.J., Wadt W.R., Ab initio effective core potentials for molecular calculations. Potentials for the transition metal atoms Sc to Hg. *J. Chem. Phys*. 82 (1985) 270-283.

Kim, K.-H., Szulejko, J. E., Raza, N., Kumar, V., Vikrant, K., Tsang, D. C. W., … Khan, A. (2019). Identifying the best materials for the removal of airborne toluene based on performance metrics - A critical review. *Journal of Cleaner Production*, 241, 118408. doi: 10.1016/j.jclepro.2019.118408

Kunaseth, M., Poldorn, P., Junkeaw, A., Meeprasert, J., Rungnim, C., Namuangruk, S., … Jungsuttiwong, S. (2017). A DFT study of volatile organic compounds adsorption on transition metal deposited graphene. *Applied Surface Science*, 396, 1712-1718. doi: 10.1016/j.apsusc.2016.11.238

Lee, C., Yang, W., Parr, R.G., Development of the Colle-Salvetti correlation-energy formula into a functional of the electron density, *Phys. Rev*. B 37 (1988) 785-789. doi:10.1103/physrevb.37.785

Mandeep, Sharma, L., & Kakkar, R. (2018). DFT study on the adsorption of p-nitrophenol over vacancy and Pt-doped graphene sheets. *Computational and Theoretical Chemistry*, 1142, 88-96. doi: 10.1016/j.comptc.2018.08.020

Suan Sunandha Science and Technology Journal

O'boyle, N. M., Tenderholt, A. L., & Langner, K. M. (2008). cclib: A library for package-independent computational chemistry algorithms. *Journal of Computational Chemistry*, 29(5), 839-845. doi: 10.1002/jcc.20823

Su, Y., Ao, Z., Ji, Y., Li, G., & An, T. (2018). Adsorption mechanisms of different volatile organic compounds onto pristine C_2N and Al-doped C_2N monolayer: A DFT investigation. *Applied Surface Science*, 450, 484-491. doi:10.1016/j.apsusc.2018.04.157

Sun, L., & Hu, J. (2018). Adsorption of O_2 on the M doped (M=Fe, Co, Al, Cu, and Zn) SiC sheets: DFT study. *Computational Condensed Matter*, 16, doi:10.1016/j.cocom.2018.e00323

Tabtimsai, C., Kansawai P., Phoson P., Pooboontong P., & Wanno B., Adsorption of CO_2 on Ga- and B-doped silicon carbide nanosheets: A theoretical study. *The 5th International Conference on Sciences and Social Sciences 2015 (ICSSS 2015): Research and Innovation for Community and Regional Development, Rajabhat Maha Sarakham University*, Thailand, September 17-18, 2015.

Tabtimsai, C., Ruangpornvisuti, V., Tontapha, S., & Wanno, B. (2018). A DFT investigation on group 8B transition metal-doped silicon carbide nanotubes for hydrogen storage application. *Applied Surface Science*, 439, 494-505.

Wadt, W.R., Hay, P.J., Ab initio effective core potentials for molecular calculations. Potentials for main group elements Na to Bi, J. Chem. Phys. 82 (1985) 284-298. doi: 10.1063/1.448799

Wang, N., Tian, Y., Zhao, J., & Jin, P. (2016). CO oxidation catalyzed by silicon carbide (SiC) monolayer: A theoretical study. *Journal of Molecular Graphics and Modelling*, 66, 196-200. doi: 10.1016/j.jmgm.2016.04.009

Yi, F.-Y., Lin, X.-D., Chen, S.-X., & Wei, X.-Q. (2008). Adsorption of VOC on modified activated carbon fiber. *Journal of Porous Materials*, 16(5), 521-526.

Yu, L., Wang, L., Xu, W., Chen, L., Fu, M., Wu, J., & Ye, D. (2018). Adsorption of VOCs on reduced graphene oxide. *Journal of Environmental Sciences*, 67, 171-178.

Zhou, K., Ma, W., Zeng, Z., Ma, X., Xu, X., Guo, Y., … Li, L. (2019). Experimental and DFT study on the adsorption of VOCs on activated carbon/metal oxides composites. *Chemical Engineering Journal*, 372, 1122-1133. doi: 10.1016/j.cej.2019.04.218

Available online at http://www.ssstj.sci.ssru.ac.th

SSSTJ

Suan Sunandha Science and Technology Journal

Conductive Composite Paper from Cellulose Fiber by in situ Polymerization of Pyrrole

Siripassorn Sukhkhawuttigit[1*], Sarute Ummartyotin[2], Yingyot Infahsaeng[1]**

[1] Division of Physics, Faculty of Science and Technology, Thammasat University, Klong Nueng, Klong Luang, Pathum-Thani, Thailand

[2] Division of Materials and Textile Technology, Faculty of Science and Technology, Thammasat University, Klong Nueng, Klong Luang, Pathum-Thani, Thailand

Corresponding author e-mail: ***ss.siripassorn@gmail.com****yingyot.infahsaeng.gmail.com**

Received: *6 January 2020* / **Revised:** *17 January 2020* /**Accepted**: *30 January 2020*

Abstract

Currently, conducting polymers such as Polypyrrole (PPy), have been extensively interested due to their interesting features of conductivity, low-cost fabrication, and stability under ambient conditions and at high temperature. Herein, polypyrrole was polymerized on the surface of cellulose fibers (CFs) by using a sequence of fiber impregnation in $FeCl_3$ solutions and re-dispersion in a pyrrole solution via in situ chemical polymerization of monomer-pyrrole. The structure, morphology, and thermal properties were investigated. The results revealed the uniformly of PPy on the surface of CFs. Moreover, conductivity of 184×10^{-4} S·cm^{-1} was obtained from a composites sheet of CFs:PPy with the PPy of 0.20 ml. Also, the decreasing of dielectric and impedance in CFs:PPy composites sheet can be observed as the increasing of CFs:PPy ratio. Chemical polymerization has been very successful in the production of composite materials of conductivity polymers with CFs.

Keywords: Polypyrrole, Conductive composite materials, in situ Synthesized

1. Introduction

Typically, the electronic devices were made of silicon, conductive glass or hard plastic, which is an importance part for high performance device, but such materials still have limitations in terms of brittleness, cost of materials and complex production processes. Moreover, some plastic, especially micro-plastic, is not environmental-friendly. Consequently, non-reused materials can lead to an environmental problem. To overcome this issue, bio-based materials have been developed under the concept of "green" and sustainable development, which can naturally decompose and pollution reduction. Therefore, the renewable natural materials are the important topic in the 21st century(Mohanty, Misra, & Drzal, 2002).

The development of alternative bio-based materials which has similar properties such as electrical, thermal, flexibility and mechanical properties, is crucial .Nowadays, the cellulose has been widely studied and developed due to its renewability, availability, non-toxicity, low-cost, biodegradability, thermal and chemical stability (Wang, Lu, & Zhang, 2016). One of the interesting developments of cellulose is conductive paper, which is very important for electronic device application such as TFT, OLED, organic photovoltaic device, stored battery, and sensor (Fu et al., 2016; Ummartyotin & Manuspiya, 2015a, 2015b). Recently, the conductive paper was successfully fabricated with a sheet resistance of 25 kΩ (Zhong et al., 2013).

To develop the conductive paper, conductive polymers are interesting material due to its unique properties that allow it to be used in a variety of electrical application. Typically, chemical polymerization has been successful in the production of composite materials of conductive polymers with the matrix. Recently, the conductive nanocrystal cellulose:polypyrrole composite hydrogel were in situ synthesized. By doping with sodium p-toluenesulfonate (TsONa), the hydrogel showed a high electrical conductivity of 8.8×10^{3} S/cm (Li, Zhang, & Xiao, 2018). Moreover, the effect of polypyrrole and ionic liquid (IL) nanocoatings on the electrical properties of cellulose film has been investigated. The conductivity of such nanocomposite film was 1.2×10^{-4} and 4.3×10^{-5} S/cm on the surface and along

the thickness direction, respectively (Mahadeva & Kim, 2011). Combination of bio-based materials such as cellulose with conductive polymer has been extensively developed as a multi-function electronic device (Du, Zhang, Liu, & Deng, 2017) . Recently, many researchers have extensively attended to develop such composite material. The organic or inorganic composite materials were a material that can be obtained from the combination of various materials to get new properties . To prepare the conductive composites of bacterial cellulose (BC) and polypyrrole, Muller and co-worker prepared through in situ oxidative chemical polymerization of pyrrole by using $FeCl_3$ as oxidant agent (Müller, Rambo, Recouvreux, Porto, & Barra, 2011). Makara and co-worker prepared nanopapers from cellulose nanofibers (CNF) and polypyrrole with high mechanical performance and with the electrical conductivity of 5.2×10^{-2} S/cm (Lay, Méndez, Delgado-Aguilar, Bun, & Vilaseca, 2016). Pyrrole and cellulose are therefore an interesting material that shows the connection between cellulose fibers and conductive polymers. There were flexibility and capacitance properties that make it more useful in using technology.

In this work, the cellulose fiber obtained from the remaining pulp is mixed with polypyrrole (PPy) via in situ polymerization using ferric chloride as oxidant agent. An amount of PPy is varied, then the morphology, mechanical, and electrical properties are investigated.

2. Materials and Method

2.1. Materials

A wastepaper pulp was provided from SCG packaging public company limited, Thailand, and was stored in a desiccator in order to prevent the moisture adsorbent .Pyrrole was supplied by Sigma Aldrich and used as received for the chemical synthesis of polypyrrole . The rest of materials, $FeCl_3$ and HCl, were also supplied by Sigma Aldrich and used without further purification.

2.2. Method

- **Cellulose suspension**

The piece of paper pulp with an area of ca. 10x10 cm^2, was ripped to be a thin sheet. Then the pulp was mixed with deionized water DI of 500 ml for overnight under magnetic stirrer .The obtained suspension was concentrated and subsequently washed with distilled water by repeated centrifuged cycles at 500 rpm. As a result, suspension of cellulose fiber (CFs) was obtained and stored at 4 ^{o}C prior to use.

- **Preparation of Cellulose fiber (CFs) and CFs:PPy paper**

CFs suspension of 45 ml (0.4 g dry weight) was dispersed in 30 ml of HCl and stirred by for 5 minutes. After that, the CFs suspension was filtered for 24 hr through a paper filter with 0.1 μm pore size and washed subsequently with DI water. The wet sheet was then dried between two membranes under an applied pressure of 0.141 psi.

For the preparation of CFs:PPy paper, the various volume of pyrrole solution (0.05, 0.10, 0.15, 0.20 ml)was dissolved in 30 ml of 0.5M HCl and, then, mixed with the CFs dispersion and stirred for 5 minutes. A defiant amount of $FeCl_3$ was dissolved in 30 ml aqueous of 0.5M HCl solution and added to the CFs:pyrrole dispersion to initiate oxidative polymerization . The oxidant ($FeCl_3$) to pyrrole was fixed at 6 %w/w ratio. The final mixture was stirred at room temperature for 30 minutes. At the end, the mixture was filtered using paper filter and washed subsequently 30 ml of 0.5M HCl and DI water to remove any small gas bubbles and to allow a better organization of CFs:PPy structures without undesired side effects, such as crystal structure damage (Ali et al., 2014).

Suan Sunandha Science and Technology Journal

2.3. Characterizations

- **Fourier Transform Infrared Spectroscopy (FTIR)**

FTIR absorption spectra (PerkinElmer, spectrum 100) of cellulose and CFs:PPy composites were recorded in the range of 4000 cm^{-1} to 650 cm^{-1} using Attenuated Reflection Infrared Spectroscopy (ATR) mode (Pleumphon, Thiangtham, Pechyen, Manuspiya, & Ummartyotin, 2017).

- **X-Ray Diffractometer (XRD)**

X-ray diffraction patterns of CFs, CFs:PPy composites were carried out by X-Ray Diffractometer (Bruker, D8 ADVANCE) using Co radiation at 40 kV voltage. The XRD patterns were recorded in a diffraction angle (2θ) range from 5° to 50° (ElNahrawy, Haroun, Hamadneh, & Al-Dujaili, 2017).

- **Thermogravimetric Analysis (TGA)**

The TGA characteristics of the CFs:PPy composite were investigated by TGA (MET-TLER TOLEDO, TGA/DSC3+1600). Each sample was heated at a heating rate of 10 °C/min under nitrogen atmosphere from room temperature to 700 °C (Pleumphon et al., 2017).

- **Field Emission Scanning Electron Microscope (FE-SEM)**

The morphological properties of the CFs and CFs:PPy composite were analyzed using FE-SEM (Hitachi, S-4800) at an acceleration voltage of 5 kV. The fiber diameter was measured and counted at 1000x magnification. Prior to the investigation, the samples were stored in desiccators to reduced humidity. Each sample was placed on carbon tape and sputtered with gold particles before being analyzed (Pleumphon et al., 2017)

- **Mechanical properties**

The sample was cuter into the rectangle shape with the width of 20 mm and length of 30 mm. The thickness of sample was ca. 0.07 - 0.09 mm. The testingspeed was 5 mm/min. The tensile tests were conducted using as Instron Universal material testing machine (Instron 55R4502, S/NH 3342) equipped with a 100 N load cell (Pleumphon et al., 2017).

- **Conductivity**

The conductivity properties of CFs:PPy substrate was characterized by Four Point Probe System (Jandel RM3000) using the cylindrical four-point probe head (Du et al., 2017).

- **Dielectric and Impedance**

Impedance were measured using an impedance probe (1260 Impedance Gain-Phaze Analyzer 12600012_Gmacd/CB Solartron) at room temperature and at various frequencies ranging from 10 Hz to 10 MHz (Jandel Engineering Limited) (ElNahrawy et al., 2017; Raghunathan, Narayanan, Poulose, & Joseph, 2017)

3. Results and discussion

3.1. FTIR analysis

The FTIR spectra of CFs and CFs:PPy composites are shown in Figure 1. The spectrum of the prepared CFs show the peaks at 3335.69 cm^{-1} which is the characteristic for stretching vibration of the hydroxyl group (O-H group) in polysaccharides (Rosa et al., 2010). The peak located at 1633 cm^{-1} correspond to stretching vibrations of C-C bonds (Poletto, Pistor, Zeni, & Zattera, 2011). The absorption bands at 1377.85, 1250.26, 1161.10, 1052.43, and 897.03 cm^{-1} belong to stretching and bending vibrations of $-CH_2$, -CH, -OH and C-O bonds in cellulose, respectively (Fackler et al., 2011; Xu, Yu, Tesso, Dowell, & Wang, 2013). From FTIR spectra of CFs:PPy composites at different PPy concentration, it was observed that the peak 3277 cm^{-1} was shifted from 3335.69 cm^{-1}, this may be due to chemical bonding between N-H in the polypyrrole ring and the –OH of cellulose (Müller et al., 2011). The fundamental vibrations of pyrrole ring observed at 1541.08 cm^{-1} and 1458 cm^{-1}, which can be assigned to the C=C and C-C ring stretching modes, respectively (Chougule et al., 2012; Hansora, Shimpi, & Mishra, 2015). The peak around 1046 cm^{-1} can be assigned to N-H in-plane deformation (Ho, Jun, & Kim, 2013), while the peak at 781 cm^{-1} is due to C-N out-of-plane deformation in PPy (Chougule et al., 2012).The absorption peak at about 1125-1159 cm^{-1} and 883.68 cm^{-1} may be relate

Vol.07, No.1 DOI:10.14456/ssstj.2020.4

Suan Sunandha Science and Technology Journal

to linkage between polypyrrole and cellulose chain in 1161.10 cm^{-1} and 867.03 cm^{-1}.

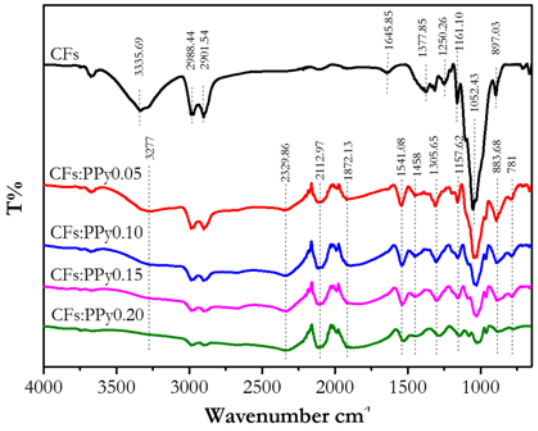

Figure 1. FTIR spectra of CFs and CFs:PPy composites.

3.2. Crystallography structures

The crystallography structures of CFs and CFs:PPy composites were characterized using XRD measurements as shown in Figure 2 .The X-ray pattern clearly exhibits the broaden peaks at 2θ of 16° and 22° for both CFs and CFs:PPy composite. The clearly peaks can be assigned to the crystalline structure of cellulose (Ford, Mendon, Thames, & Rawlins, 2010). Also, the broaden characteristic of various CFs:PPy composites were exhibited in the region of 15° - 25° which is the amorphous phase of polypyrrole (Luo et al., 2010).

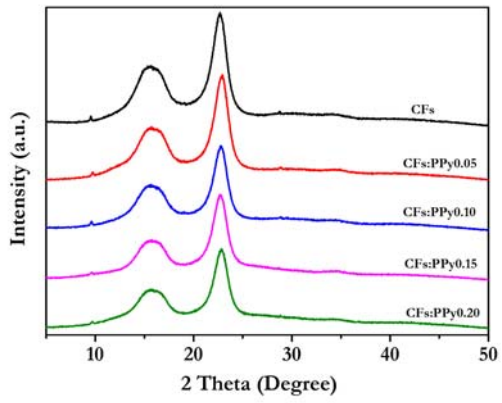

Figure 2. XRD patterns of CFs and CFs:PPy composites.

3.3. Thermogravimetric analysis

The degradation temperatures of CFs and CFs:PPy papers were studied by thermogravimetric analysis as shown in Figure 3. CFs and CFs:PPy showed main weight loss in three stages. For CFs, it demonstrates that the thermal stability of the prepared CFs in much higher than that of composites in the temperature lower than 250 ℃. As composite is hygroscopic, nearly 8% weight loss is occurred at 100 ℃. The second stage of weight loss started at 250 ℃ and continued up to 500 ℃ with rapidly 80% of weight loss. The last stages of temperature at > 500 ℃ almost 100% of weight loss can be observed for all conditions. For CFs:PPy composites, the first stage range between room temperature and 250 ℃ showed about a 13% of weight loss. The second stage of weight loss started at 250 ℃ and continued up to 500 ℃ during which there was nearly an 80% of gradually weight loss. The last states of temperature up to 500 ℃ during which there was a 100% of weight loss. From the above analysis, it clearly shows that the thermal stability of CFs was greatly affected by incorporating PPy. The incorporated PPy lowered the starting thermal degradation of CFs.

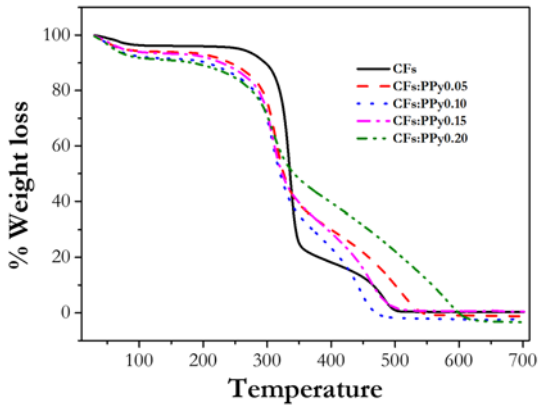

Figure 3. TGA of CFs and CFs:PPy composites.

3.4. FE-SEM analysis

The morphology of CFs, CFs:PPy composites was studied using Field Emission Scanning Electron Microscope as shown in Figure 4. The Figure 4 (a) shown that the CFs surface is rather straight and smooth without the formation of cross-link between fiber. It is important to note that CFs appears to be a

Vol.07, No.1 DOI: 10.14456/ssstj.2020.4

Suan Sunandha Science and Technology Journal

uniform fibrous network. For CFs:PPy composites as shown in Figure 4 (b-e), the formation of PPy on the CFs in the form of clusters and cross-link between fiber network can be observed (ElNahrawy et al., 2017), which involving the formation of H-bonds between the cellulose and the polypyrrole chain. These interactions were a result of both intermolecular and intramolecular forces, causing the composites sheet to be less cellulose fiber density.

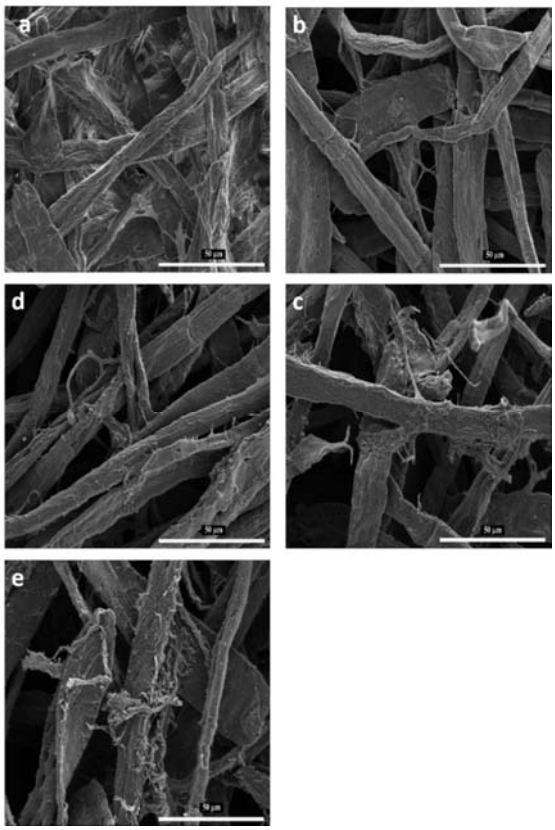

Figure 4. FE-SEM of composite materials with different pyrrole preparation condition (a) CFs (b) CFs:PPy0.05 (c) CFs:PPy0.10 (d) CFs:PPy0.15 (e) CFs:PPy0.20.

3.5. Mechanical properties

The tensile strength, Young's modulus, and elongation at break of neat CFs and CFs:PPy composite were presented in Table 1. Not surprisingly, tensile strength and young's modulus were decreased as the increasing of PPy additive. This effect may be caused by the inter-percolation of PPy between CFs network. However, the elongation at break of composite is not dramatically reduced, when increasing the amount of additive. After the polymerization process of pyrrole, PPy network may be grouped to be clusters which can be observed from the SEM image. Therefore, PPy network was poorly dispersed into cellulose fibers matrix by present preparation.

Table 1. Mechanical properties of CFs and CFs:PPy composites.

Sample	Tensile strength (MPa)	Young's modulus (MPa)	Elongation at break (%)
CFs	2.038±0.761	248.940±85.926	1.404± 0.440
CFs:PPy0.05	0.798±0.520	109.652±871.73	1.180±0.234
CFs:PPy0.10	0.554±0341	109.858±68.977	0.698±0.119
CFs:PPy0.15	0.213±0.285	39.715±53.154	0.868±0.331
CF:PPy0.20	0.026±0.020	2.962±3.546	1.524±0.389

3.6. Conductivity properties

The electrical conductivities of CFs:PPy composites with different amount of PPy were measured using a four-point probe technique. Table 2 shows the sheet resistance, resistivity, and electrical conductivities of CFs:PPy composites. The experimental setup and parameters calculation are described in literature (J. Li, Wang, & Ba, 2012). The CFs has basically no conductivity, while the resistance and resistivity of CFs:PPy composites decrease as the increasing of PPy additive. Consequently, the electrical conductivities of CFs:PPy composites are increased up to 1.84×10^{-2} S/cm at 0.20 ml PPy. Compare to the conductivity of typically semiconductor (10^{-7}–10^{5} S/cm), the conductivity of CFs:PPy is in a range of promising application of electronic device.

Vol.07, No.1 DOI:10.14456/ssstj.2020.4

Suan Sunandha Science and Technology Journal

Table 2. Conductivity of the CFs and CFs:PPy composites.

Sample	Resistance (Ω) x10^3	Resistivity (Ωm) x10^3	Conductivity (S·cm^{-1})x10^{-4}
CFs	-	-	-
CFs:PPy(0.05)	10.7±0.742	67.4±4.66	1.49±0.106
CFs:PPy(0.10)	1.19±0.0944	7.51±0593	13.3±1.05
CFs:PPy(0.15)	0.735±0.0792	4.62±0.498	21.9±2.44
CFs:PPy(0.20)	0.0938±0.0241	0.589±0.151	184±58.9

3.7. Dielectric properties

Figure. 5. Shows dielectric properties of CFs and CFs:PPy composite materials. Typically, the dielectric properties of polymer composites can be affected by the polymer type or dopant type. The variation of dielectric constant (permittivity, ε′) and loss tangent as a function of frequency for the prepared samples with different composition of PPy are presented. The dielectric constants were very high at low frequency and were slightly decreased when the frequency increased. Note that the dielectric constant of CFs is more rapidly decreased when comparing to that of CFs:PPy composites. The reducing of dielectric constants can be expressed by the relaxation behavior. With high region of frequency, the charge has insufficient time of re-orientation under applied external field and it was therefore presented as a lower of dielectric properties. In addition, the loss tangent of CFs and CFs:PPy composite is not significantly difference.

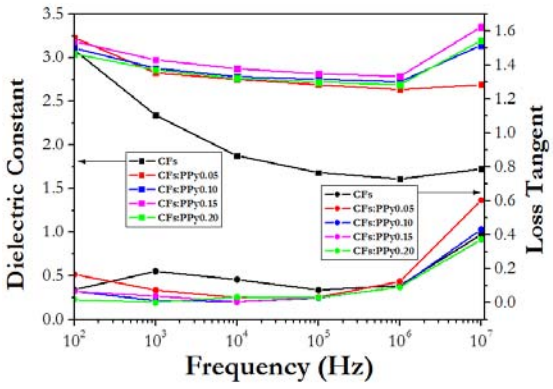

Figure 5. Variation of dielectric constant and loss tangent of CFs and CFs:PPy composites with frequency.

3.8. Impedance properties

Figure. 6. Shows the complex impedance spectra with the variation of the imaginary part of the complex impedance (Z″) versus its real part (Z′). The frequency range was from 10 Hz to 10 MHz and the applied AC signal was 0.5 V. The impedance spectra are characterized as semicircle, which is most probably result of the facilitated transport of the doping anions in the bulk of the composites. The transport of the doping anions can be enhance by increasing the amount of PPy (Nakata & Kise, 1993; Porjazoska Kujundjiski, Chamovska, & Grchev, 2014). The best fit of experimental data to model was obtained using a constant phase element (CPE) rather than an ideal capacitor. The equivalent circuit model is shown in Figure 6. The best fit of experimental data to model was obtained using a constant phase element (CPE) rather than an ideal capacitor. The capacitance of 3.168×10^{-11} F can be obtained from the composites at 0.20 ml PPy. The equivalent circuit model is shown in Figure 6.

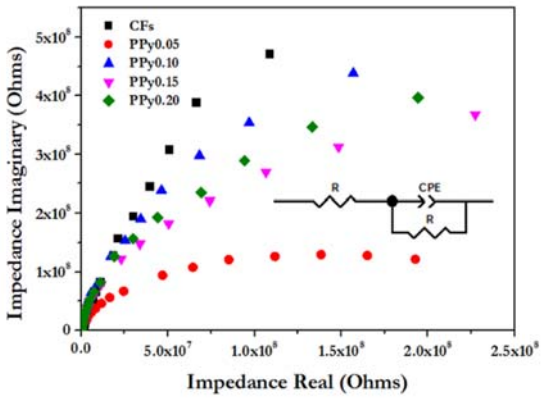

Figure 6. Figure 6. Impedance spectra of CFs and CFs:PPy composites.

4. Conclusions

A cellulose paper was demonstrated with the aid of in situ synthesized conductive cellulose (CFs):polypyrrole (PPy) network. Chemical polymerization has been very successful in the production of composite materials of conductivity polymers with CFs. Increasing polypyrrole content in the composite affected the features of cellulose. The morphology of CFs exhibited a very straight and smooth surface. When PPy was composited with

Vol.07, No.1 DOI:10.14456/ssstj.2020.4

Suan Sunandha Science and Technology Journal

CFs, the PPy clusters were formed on the CFs. Increasing of the PPy amount causes the reduction of mechanical properties due to interpercolation of PPy in cellulose. Also, the decreasing of dielectric and impedance in CFs:PPy composites sheet can be observed as the increase of CFs:PPy ratio. Moreover, conductivity of 184×10^{-4} S/cm was obtained from a composites sheet of CFs:PPy (0.20).

5. Acknowledgement

The authors would like to thank for the financial support provided by Thammasat University under the National Research Council of Thailand (NRCT)

6. Publication Ethic

Submitted manuscripts must not have been previously published by or be under review by another print or online journal or source.

7. References

Ali, F., Reinert, L., Lévêque, J.-M., Duclaux, L., Muller, F., Saeed, S., & Shah, S. S. (2014). Effect of sonication conditions: solvent, time, temperature and reactor type on the preparation of micron sized vermiculite particles. *Ultrasonics sonochemistry, 21*(3), 1002-1009. doi: 10.1016/j.ultsonch.2013.10.010

Chougule, M., Dalavi, D., Mali, S., Patil, P., Moholkar, A., Agawane, G., . . . Patil, V. (2012). Novel method for fabrication of room temperature polypyrrole–ZnO nanocomposite NO2 sensor. *Measurement, 45*(8), 1989-1996. doi: 10.1016/j.measurement.2012.04.023

Du, X., Zhang, Z., Liu, W., & Deng, Y. (2017). Nanocellulose-based conductive materials and their emerging applications in energy devices-A review. *Nano Energy, 35*, 299-320. doi:10.1016/j.nanoen.2017.04.001

El Nahrawy, A. M., Haroun, A. A., Hamadneh, I., & Al-Dujaili, A. H. (2017). Conducting cellulose/TiO_2 composites by in situ polymerization of pyrrole. *Carbohydrate polymers, 168*, 182-190. doi: 10.1016/j.carbpol.2017.03.066

Fackler, K., Stevanic, J. S., Ters, T., Hinterstoisser, B., Schwanninger, M., & Salmén, L. (2011). FT-IR imaging microscopy to localise and characterise simultaneous and selective white-rot decay within spruce wood cells. *Holzforschung, 65*(3), 411-420.

Ford, E. N. J., Mendon, S. K., Thames, S. F., & Rawlins, J. W. (2010). X-ray diffraction of cotton treated with neutralized vegetable oil-based macromolecular crosslinkers. *Journal of Engineered Fibers and Fabrics, 5*(1), 155892501000500102. doi:10.1177/155892501000500102

Fu, J., Zhang, J., Song, X., Zarrin, H., Tian, X., Qiao, J., . . . Chen, Z. (2016). A flexible solid-state electrolyte for wide-scale integration of rechargeable zinc–air batteries. *Energy & Environmental Science, 9*(2), 663-670. doi:10.1039/c5ee03404c

Hansora, D., Shimpi, N., & Mishra, S. (2015). Graphite to graphene via graphene oxide: an overview on synthesis, properties, and applications. *Jom, 67*(12), 2855-2868. doi: 10.6084/m9.figshare.1094371

Ho, T. A., Jun, T.-S., & Kim, Y. S. (2013). Material and NH_3-sensing properties of polypyrrole-coated tungsten oxide nanofibers. *Sensors and Actuators B: Chemical, 185*, 523-529. doi:10.1016/j.snb.2013.05.039

Lay, M., Méndez, J. A., Delgado-Aguilar, M., Bun, K. N., & Vilaseca, F. (2016). Strong and electrically conductive nanopaper from cellulose nanofibers and polypyrrole. *Carbohydrate polymers, 152*, 361-369. doi:10.1016/j.carbpol.2016.06.102

Li, J., Wang, Y., & Ba, D. (2012). Characterization of semiconductor surface conductivity by using microscopic four-point probe technique. *Physics Procedia, 32*, 347-355. doi: 10.1016/j.phpro.2012.03.568

Li, Y., Zhang, H., Ni, S., & Xiao, H. (2018). In situ synthesis of conductive nanocrystal cellulose/polypyrrole composite hydrogel based on semi-interpenetrating network. *Materials Letters, 232*, 175-178.

Luo, Y.-L., Fan, L.-H., Xu, F., Chen, Y.-S., Zhang, C.-H., & Wei, Q.-B. (2010). Synthesis and characterization of Fe_3O_4/PPy/P (MAA-co-AAm) trilayered composite microspheres with electric, magnetic and pH response characteristics. *Materials Chemistry and Physics, 120*(2-3), 590-597.

Mahadeva, S. K., & Kim, J. (2011). Enhanced electrical properties of regenerated cellulose by polypyrrole and ionic liquid nanocoating. *Proceedings of the Institution of Mechanical Engineers, Part N: Journal of Nanoengineering and Nanosystems, 225*(1), 33-39. doi:10.1177/1740349911404100

Mohanty, A. K., Misra, M., & Drzal, L. (2002). Sustainable bio-composites from renewable resources: opportunities and challenges in the green materials world. *Journal of Polymers and the Environment, 10*(1-2), 19-26.

Müller, D., Rambo, C., Recouvreux, D., Porto, L., & Barra, G. (2011). Chemical in situ polymerization of polypyrrole on bacterial cellulose nanofibers. *Synthetic Metals, 161*(1-

Suan Sunandha Science and Technology Journal

2),106-111. doi:10.1016/j.synthmet.2010.11.005

Nakata, M., & Kise, H. (1993). Preparation of Polypyrrole-Poly(vinyl chloride) Composite Films by Interphase Oxidative Polymerization. *Polymer Journal, 25*(1), 91-94. doi:10.1295/polymj.25.91

Pleumphon, C., Thiangtham, S., Pechyen, C., Manuspiya, H., & Ummartyotin, S. (2017). Development of conductive bacterial cellulose composites: An approach to bio-based substrates for solar cells. *Journal of Biobased Materials and Bioenergy, 11*(4), 321-329.doi: 10.1166/jbmb.2017.1686

Poletto, M., Pistor, V., Zeni, M., & Zattera, A. J. (2011). Crystalline properties and decomposition kinetics of cellulose fibers in wood pulp obtained by two pulping processes. *Polymer Degradation and Stability, 96*(4), 679-685. doi:10.1016/j.polymdegradstab.2010.12.007

Porjazoska Kujundjiski, A., Chamovska, D., & Grchev, T. (2014). Capacitive properties of polypyrrole/activated carbon composite. *Hemijska industrija, 68*, 63-63. doi:10.2298/HEMIND140305063P

Raghunathan, S. P., Narayanan, S., Poulose, A. C., & Joseph, R. (2017). Flexible regenerated cellulose/polypyrrole composite films with enhanced dielectric properties. *Carbohydrate polymers, 157*, 1024-1032. doi: 10.1016/j.carbpol.2016.10.065

Rosa, M., Medeiros, E., Malmonge, J., Gregorski, K., Wood, D., Mattoso, L., . . . Imam, S. (2010). Cellulose nanowhiskers from coconut husk fibers: Effect of preparation conditions on their thermal and morphological behavior. *Carbohydrate polymers, 81*(1), 83-92. doi: 10.1016/j.carbpol.2010.01.059

Ummartyotin, S., & Manuspiya, H. (2015a). A critical review on cellulose: from fundamental to an approach on sensor technology. *Renewable and Sustainable Energy Reviews, 41*, 402-412. doi: 10.1016/j.rser.2014.08.050

Ummartyotin, S., & Manuspiya, H. (2015b). An overview of feasibilities and challenge of conductive cellulose for rechargeable lithium based battery. *Renewable and Sustainable Energy Reviews, 50*, 204-213. doi:10.1016/j.rser.2015.05.014

Wang, S., Lu, A., & Zhang, L. (2016). Recent advances in regenerated cellulose materials. *Progress in Polymer Science, 53*, 169-206. doi:10.1016/j.progpolymsci.2015.07.003

Xu, F., Yu, J., Tesso, T., Dowell, F., & Wang, D. (2013). Qualitative and quantitative analysis of lignocellulosic biomass using infrared techniques: a mini-review. *Applied Energy, 104*,801-809. doi:10.1016/j.apenergy.2012.12.019

Zhong, Q., Zhong, J., Hu, B., Hu, Q., Zhou, J., & Wang, Z. L. (2013). A paper-based nanogenerator as a power source and active sensor. *Energy & Environmental Science, 6*(6), 1779-1784. doi: 10.1039/c3ee40592c

Available online at http://www.ssstj.sci.ssru.ac.th

Suan Sunandha Science and Technology Journal

Stratified Unified Ranked Set Sampling for Asymmetric Distributions

Chainarong Peanpaylun[1*], Chanankarn Saengprasan[1], Suwiwat Witchakool[1]

[1]Department of Mathematics and Statistics, Faculty of Science and Technology,
Sakon Nakhon Rajabhat University, Sakon Nakhon 47000, Thailand

Corresponding author e-mail: *tankku555@gmail.com

Received: *6 January, 2020* / **Revised:** *17 January 2020* / **Accepted**: *30 January 2020*

Abstract

The purposes of this study are to propose a modified ranked set sampling, which is called stratified unified ranked set sampling (SURSS), for estimating the population mean and compare the efficiency of the empirical mean estimator based on SURSS with their counterparts in simple random sampling (SRS), stratified simple random sampling (SSRS), and stratified ranked set sampling (SRSS) via a simulation. We compare efficiency using criteria mean square error (MSE) and simulate the data from three asymmetric distributions: Exponential (1), Geometric (0.5), and Gamma (1, 2). It is found that the estimator in SURSS provides more efficient than their counterparts in SRS, SSRS, and SRSS for three parent asymmetric distributions with small sample size. For the larger sample size, the proposed estimator in SURSS still provide more efficient than SRS, but it gives more efficient than SSRS and SRSS in some cases.

Keywords: simple random sampling, ranked set sampling, unified ranked set sampling, stratified unified ranked set sampling

1. Introduction

In 1952, McIntyre (1952) proposed a ranked set sampling (RSS) method to estimate the population mean of average yields. Later, RSS was developed and modified by many authors to estimate the population parameters. In 1968, Takahasi and Wakimoto (1968) provided the mathematical proof for RSS. They proved that the sample mean based on RSS is an unbiased estimator of the population mean which gave smaller variance than the sample mean based on a simple random sample (SRS) with the same sample size. In 1972, Dell and Clutter (1972) demonstrated that the variance of the sample mean based on RSS is less than or equal to that of the SRS, whether or not there are errors in ranking. In 1996, Samawi (1996) suggested a stratified ranked set sampling (SRSS). In 2011, Mustafa, Al-Nasser, and Aslam (2011) introduced a folded ranked set sampling for asymmetric distributions. In 2017, Matthews and Wolfe (2017) suggested a unified ranked sampling (URSS). The RSS method is efficiency increasing the number of set and the number of cycles.

The aim of this study are to propose the stratified unified ranked set sampling (SURSS) for estimating the population mean of asymmetric distributions and to study the efficiency of the empirical mean estimator based on SURSS.

2. Materials and methods

2.1 Simple Random Sampling (SRS)

SRS is a method of selecting n units out of N units such that every one of the ${}_{N}C_{n}$ distinct samples has an equal chance of being drawn.

2.2 Stratified Sampling

In stratified sampling method, the population of N units is divided into L non overlapping sub-groups known as strata each stratum has $N_1, N_2, ..., N_L$ units, respectively, such that $N_1 + N_2 + ... + N_L = N$. For full benefit from stratification, the size of the h^{th} strata, denoted by N_h for $h = 1, 2, ..., L$, must be known. Then the samples are drawn independently from each stratum, producing samples sizes denoted by $n_1, n_2, ..., n_L$, such that the total sample size is $n = \sum_{h=1}^{L} n_h$. If a simple random sample is taken from each stratum,

Vol.07, No.1 DOI: 10.14456/ssstj.2020.5

Suan Sunandha Science and Technology Journal

the whole procedure is known as **a stratified simple random sampling** (**SSRS**).

2.3 Ranked Set Sampling (RSS)

RSS technique can be described as follows:

Step 1: Use a SRS method to select m^2 units from the population of interest.

Step 2: Allocate the m^2 selected units randomly into m sets, each of size m.

Step 3: Rank the m units in each set with respect to the variable of interest.

Step 4: Choose a sample by taking the smallest ranked unit in the first set, the second smallest ranked unit in the second set, continue the process until the largest ranked unit is selected from the last set. Then the taken samples are measured the variable of interest.

Step 5: Repeat step 1 through step 4 for r cycles to draw the RSS sample of size $n = mr$.

(Al-Omari & Bouza, 2014, pp. 215-235)

2.4 Unified Ranked Set Sampling (URSS)

URSS technique can be described as follows:

Step 1: Use a SRS method to select m^2 units from the population of interest and rank them with respect to the variable of interest.

Step 2: Select the sample units for measurement as follow

If m is an odd number, the ranked $\left(\frac{m+1}{2}+(i-1)m\right)^{th}$ units will be selected for $i = 1,2,...,m$. On the other hands, if m is an even number, the ranked $\left(\frac{m}{2}+(i-1)m\right)^{th}$ units will be selected, for $i = 1,2,...,m$.

Step 3: Repeat steps 1 and 2 for r cycles (for $j = 1,2,...,r$) to draw the URSS of size $n = mr$.

Define $X_{[i]j}$ be the URSS sampled unit of the i^{th} rank from the j^{th} cycle, where $i = 1,2,...,m$ and $j = 1,2,...,r$.

(Zamanzade, 2014)

2.5 Stratified Unified Ranked Set Sampling (SURSS)

The population of N units is divided into L non overlapping sub-groups known as strata each stratum have $N_1, N_2, ..., N_L$ units, respectively, such that $N_1 + N_2 + ... + N_L = N$. The size of the h^{th} strata denotes by N_h for $h = 1,2,...,L$. Then the samples are drawn independently from each stratum, producing samples sizes denoted by $n_1, n_2, ..., n_L$, such that the total sample size is $n = \sum_{h=1}^{L} n_h$. If the URSS technique is applied for each stratum then the whole procedure is called a SURSS. Define $X^h_{[i]j}$ be the SURSS sampled unit of the i^{th} rank, the j^{th} cycle in the h^{th} stratum, where $i = 1,2,...,m$; $j = 1,2,...,r$; and $h = 1,2,...,L$. The mean of selected units is used as a population mean estimator.

To compare the efficiency of the empirical mean estimator based on SURSS with their counterparts in SRS, SSRS, and SRSS via a simulation in RStudio under the population of 100,000 units divided into two strata each stratum has 50,000 units with the numbers of set in each stratum $m = 2,5,10$ and the number of cycles $r = 2,5,10$.

3. Results and Discussions

3.1 Estimation of Population Mean

Let $X_1, X_2, ..., X_n$ be n independent random variables from a probability density function $f(x)$, with mean (μ) and variance (σ^2). The empirical mean estimator of URSS is given by

$$\bar{X}_{URSS} = \frac{1}{mr}\sum_{i=1}^{m}\sum_{j=1}^{r} X_{\lceil l+(i-1)m \rceil j} \quad (1)$$

where $l = \frac{m}{2}$ if i is an even number and $l = \frac{m+1}{2}$ if i is an odd number (for $i = 1,2,...,m$).

The URSS variance can be estimated by

$$S^2_{URSS} = \frac{1}{mr-1}\left\{\sum_{i=1}^{m}\sum_{j=1}^{r}\left(X_{\lceil l+(i-1)m \rceil j} - \bar{X}_{URSS}\right)^2\right\}. \quad (2)$$

Vol.07, No.1 DOI: 10.14456/ssstj.2020.5

Suan Sunandha Science and Technology Journal

The SURSS estimator of the population mean is given by

$$\bar{X}_{SURSS} = \sum_{h=1}^{L} W_h \left(\bar{X}^h_{URSS} \right) \qquad (3)$$

where $W_h = \frac{N_h}{N}$ and $\bar{X}^h_{URSS}$ is the URSS mean estimator in the h^{th} stratum.

The variance of $\bar{X}_{SURSS}$ is given by

$$\begin{aligned} Var\left(\bar{X}_{SURSS}\right) &= Var\left[\sum_{h=1}^{L} \frac{W_h}{m_h r}\left(\sum_{i=1}^{m_h}\sum_{j=1}^{r} X_{[l+(i-1)m_h]j}\right)\right] \\ &= \sum_{h=1}^{L} \frac{W_h^2}{m_h^2 r^2}\left(\sum_{i=1}^{m_h}\sum_{j=1}^{r} Var\left(X_{[l+(i-1)m_h]j}\right)\right) \\ &= \sum_{h=1}^{L} \frac{W_h^2}{m_h^2 r^2}\left(\sum_{i=1}^{m_h}\sum_{j=1}^{r} \sigma^2_{[l+(i-1)m_h]j,h}\right) \\ &= \sum_{h=1}^{L} \frac{W_h^2}{m_h r} \sigma^2_{[l+(i-1)m_h]j,h} \qquad (4) \end{aligned}$$

3.2 Simulation Study

The simulation study is designed to investigate the performance of SURSS for estimating the population mean compared to their counterparts in SRS, SSRS, and SRSS under asymmetric distributions: Exponential(1), Geometric(0.5), and Gamma(1, 2). The simulations are done based on the population of 100,000 units is divided into two strata each stratum has 50,000 units, which are conducted for the numbers of set in each stratum $m = 2,5,10$ and the number of cycles $r = 2,5,10$ on 5,000 replications. If the underlying distribution is asymmetric, the efficiencies of SURSS relative to SRS, SSRS, and SRSS, respectively are given by

$$eff\left(\bar{X}_{SURSS}, \bar{X}_{SRS}\right) = \frac{MSE\left(\bar{X}_{SRS}\right)}{MSE\left(\bar{X}_{SURSS}\right)},$$

$$eff\left(\bar{X}_{SURSS}, \bar{X}_{SSRS}\right) = \frac{MSE\left(\bar{X}_{SSRS}\right)}{MSE\left(\bar{X}_{SURSS}\right)},$$

$$eff\left(\bar{X}_{SURSS}, \bar{X}_{SRSS}\right) = \frac{MSE\left(\bar{X}_{SRSS}\right)}{MSE\left(\bar{X}_{SURSS}\right)},$$

where MSE is the mean square error (MSE).
The simulation results are shown in Tables 1-3.

Table 1. The efficiency of SURSS relative to SRS, SSRS, and SRSS for estimating the population mean with $m = 2$ and $r = 2,5,10$

Distribution	r	Efficiency		
		SURSS vs. SRS	**SURSS vs. SSRS**	**SURSS vs. SRSS**
Exp(1)	2	**4.5738**	**2.3453**	**1.1372**
	5	**2.4891**	**1.2585**	0.3571
	10	**1.0906**	0.5499	0.0990
Geo(0.5)	2	**4.6105**	**2.3540**	**1.1868**
	5	**2.4206**	**1.2129**	0.3565
	10	**1.0614**	0.5784	0.0998
Gamma (1,2)	2	**4.5327**	**2.2916**	**1.2159**
	5	**2.2539**	**1.2350**	0.3530
	10	**1.0749**	0.5506	0.1024

Based on Table 1, the numbers of set in each stratum $m = 2$, it indicates that the SURSS estimator is more efficient than SRS estimator for all numbers of cycle $r = 2,5,10$ based on all three asymmetric distributions. In addition, the SURSS estimator is more efficient compared to SSRS for $r = 2,5$ based on all three asymmetric distributions. Moreover, the SURSS estimator is more efficient than SRSS estimator for $r = 2$ based on all three asymmetric distributions.

Table 2: The efficiency of SURSS relative to SRS, SSRS, and SRSS for estimating the population mean with $m = 5$ and $r = 2,5,10$

Distribution	r	Efficiency		
		SURSS vs. SRS	**SURSS vs. SSRS**	**SURSS vs. SRSS**
Exp(1)	2	**2.3324**	**1.2083**	0.3523
	5	0.8265	0.4251	0.0641
	10	0.3998	0.2073	0.0185
Geo(0.5)	2	**2.2595**	**1.2333**	0.3529
	5	0.8600	0.4372	0.0658
	10	0.3966	0.2112	0.0186
Gamma (1,2)	2	**2.4353**	**1.2216**	0.3608
	5	0.8246	0.4408	0.0661
	10	0.3973	0.2066	0.0185

Based on Table 2, the numbers of set in each stratum $m = 5$, we can conclude that the

Vol.07, No.1 DOI: 10.14456/ssstj.2020.5

Suan Sunandha Science and Technology Journal

SURSS estimator is more efficient compared to SRS and SSRS estimators for the numbers of cycle $r = 2$ based on all three asymmetric distributions.

Table 3. The efficiency of SURSS relative to SRS, SSRS, and SRSS for estimating the population mean with $m = 10$ and $r = 2,5,10$

Distribution	r	Efficiency		
		SURSS vs. SRS	**SURSS vs. SSRS**	**SURSS vs. SRSS**
Exp(1)	2	**1.0782**	0.5517	0.1029
	5	0.3957	0.2094	0.0187
	10	0.1987	0.0976	0.0049
Geo(0.5)	2	**1.0620**	0.5499	0.1002
	5	0.3882	0.2150	0.0188
	10	0.1927	0.1036	0.0047
Gamma (1,2)	2	**1.0815**	0.5694	0.0953
	5	0.3985	0.2110	0.0178
	10	0.2034	0.1031	0.0049

Based on Table 3, the numbers of set in each stratum $m = 10$, it implies that the SURSS estimator is more efficient than SRS estimators for the numbers of cycle $r = 2$ based on all three asymmetric distributions.

4. Conclusion

In conclusion, the proposed estimator in SURSS provide more efficient than their counterparts in SRS, SSRS, and SRSS for three parent asymmetric distributions in the case of a small sample size. For the larger sample size, the proposed estimator in SURSS still provide more efficient than SRS, but it gives more efficient than SSRS and SRSS in some cases.

5. Acknowledgement

This work was partially funded by the National Research Council of Thailand (NRCT). The authors would like to express our thanks to Research and Development Institute, Sakon Nakhon Rajabhat University and the Department of Mathematics and Statistics, the Faculty of Science and Technology, Sakon Nakhon Rajabhat University. We also thank the referees and the associate editor for their useful comments and suggestions on the earlier draft that led to this improved version.

6. Publication Ethic

Submitted manuscripts must not have been previously published by or be under review by another print or online journal or source.

7. References

Al-Omari, A.I., & Bouza, C.N. (2014). Review of Ranked Set Sampling: Modifications and Applications. *Revista Investigacion Operacional, 35*(3), 215-235.

Dell, T.R., & Clutter, J.L. (1972). Ranked Set Sampling Theory with Order Statistics Background. *Biometrics*, 28, 545–555. doi: 10.2307/2556166

Matthews, M.J. & Wolfe, D.A. (2017). Unified Ranked Sampling. *Statistics & Probability Letters*, *112*(C), 173–178. doi: 10.1016/j.spl.2016.11.015

McIntype, G.A. (1952). A Method of Unbiased Selective Sampling Using Ranked Sets. *Australian Journal of Agricultural Research, 3*(4), 385-390. doi:10.1071/AR9520385

Mustafa, A.B., Al-Nasser, A.D., & Aslam, M. (2011). Folded Ranked Set Sampling for Asymmetric Distributions. *Communications of the Korean Statistical Society, 18*(1), 147–153. doi:10.5351/ckss.2011.18.1.147

Samawi, H. M. (1996). Stratified ranked set sample, *Pakistan Journal of Statistics, 12*(1), 9-16.

Takahasi, K., & Wakimoto, K. (1968). On Unbiased Estimates of the Population Mean Based on the Sample Stratified by Means of Ordering. *Annals of the Institute of Statistical Mathematics*, 20, 1-31.

Zamanzade, E. (2014). Unified Ranked Set Sampling. Retrieved from https://arxiv.org/vc/arxiv/papers/1411/1411.1351v1.pdf

Available online at http://www.ssstj.sci.ssru.ac.th

SSSTJ

Suan Sunandha Science and Technology Journal

Development of High Anthocyanin Crispy Rice Bar

Nuttawut Lainumngen[1*], Janpen Saengprakai[1], Siriporn Tanjor[1], Wasan Phanpho[2], Aran Phodsoongnoen[2]

[1]Department of Nutrition and Health, Institute of Food Research and Product Development, Kasetsart University, Bangkok 10903, Thailand
[2]Faculty of Agro-industrial Technology, Rajamangala University of Technology Tawan-ok, Chanthaburi 22210, Thailand
*Corresponding author e-mail: ifrnwl@ku.ac.th

Received: 6 ***January*** *2020* / **Revised:** *17 January 2020* / **Accepted**: *30 January 2020*

Abstract

Nowadays, consumers are increasingly interested in healthy food. This study aimed to increase the nutritional value of crispy rice by using Thai rice which presented important natural ingredients. Five formulations were developed including Thai colored indica rice (*Oryza sativa* cv. Riceberry), black sticky rice (*Oryza sativa* cv. Leum Phua), white glutinous rice (*Oryza sativa* cv. RD6), RD6 soaking in water obtained from Leum Phua sticky rice, and a combination of RD6 and Leum Phua glutinous rice. Water activity, moisture content, crispness, color, total anthocyanin content, and sensory evaluation were analyzed. The results showed that there was no significant difference in crispness and moisture content of products. The lowest free water was observed in both Riceberry and soaked RD6 formulations with water activity below 0.42. Leum Phua and Riceberry recipes had the lowest brightness. Obviously, crispy rice bar from Leum Phua sticky rice had the highest total anthocyanin content, followed by Riceberry rice. According to sensory test, the color score was high in the RD6 and soaked RD6 formulations. During the storage for 2 months, the increase of water activity and lipid peroxidation were observed. However, there was no growth of pathogenic microorganisms. The crispy rice by soaked RD6 formula was acceptable up to 2 months of storage. Therefore, it can be concluded that the RD6 sticky rice soaking with water from black glutinous rice is suitable for commercial production because it can increase the nutritional value for consumers by providing high total anthocyanin content. 3456789

Keywords: Riceberry rice, Leum Phua rice, RD6 rice, Black glutinous rice, Anthocyanin

1. Introduction

Many studies have been pointing out to the critical issue of food eating awareness related to physical illness throughout the past few decades. Eating behavior is an important factor that impacts on human health. Thus, healthier food choice is recommended for healthy consumers. In the present, human lifestyle has been completely changed to hurry in living which directly influences trend of food decision as well as their dietary pattern consumption. Food characteristics, suitable for people who living in a hurry each day, should be ready-to-eat and easy-to-carry such as sandwiches, bread and snacks. Importantly, making decision of eating food must include both healthy and safe as the priority. In present, people are facing a challenge to develop nutritious food product which fit in daily lifestyle. Therefore, this ongoing issue causes of global food industry focusing on functional ingredients from natural plants for developing healthier products. Hence, utilization of anthocyanin-based food is needed to add the value in food products and also enriched nutrition in food with natural source.

Thailand is well known as the land of agriculture, especially rice cultivation in different strains with high quality. Thai colored indica rice (*Oryza sativa* cv. Riceberry), black glutinous rice (*Oryza sativa* cv. Leum Phua) and white glutinous rice (*Oryza sativa* cv. RD6) have been cultivated widely in Thailand. Interestingly, pigmented rice contains phytonutrient which is higher antioxidant activity and phenolic compounds than non-pigmented rice. Several varieties of pigmented rice, particularly Riceberry

rice and Leum Phua sticky rice have been exhibited as source of anthocyanin. It is water-soluble, phenolic of plant which contributes to red, purple or blue colors in rice. Anthocyanin-based food products have been developing for healthier choice. It has becoming popular in food and beverage research, such as substitution of Riceberry flour in noodle and fortification of anthocyanin from Riceberry rice in milk chocolate (Sirichokworrakit, Phetkhut, & Khommoon, 2015; Ngamdee, Bunnasart, & Sonda, 2019). Moreover, effect of anthocyanin has been reported as a potent nutraceutical by its antioxidant capacity. Health benefits were reported in previous literature that mainly involved in anti-oxidative stress and anti-inflammation throughout the body. Furthermore, pharmacological effect of anthocyanin in Thai rice as anti-hyperlipidemic and anti-cancer property have been reported. (Khoo, Azlan, Tang, & Lim, 2017; Sivamaruthi, Kesika, & Chaiyasut, 2018). Glutinous rice can be modified in many kinds of food such as snack or dessert. Leum Phua and RD6 are Thai glutinous rice with pigmented and non-pigmented carrier, respectively. Leum Phua, black glutinous rice, has been reported that it exhibited high anthocyanin profile, phenolic compounds and radical scavenging activity than Black Rose, Hawm Nil, and Klam rice (Suwannalert & Rattanachittawat, 2011). White glutinous rice RD6 is one of the popular rice grown in Thailand. It is commonly modified and developed to snack or cake due to puffable property even though lower antioxidant activity is exhibited when compared to other colored Thai rice.

Recently, Thai rice containing anthocyanin has been widely studied due to rise of concern in healthier eating habits. The application of natural material on Thai traditional snack is still needed. In addition, to our knowledge, the comparison of pigmented rice utilization in snack bar is rarely observed. Therefore, the objective of this study was to increase the nutritional value of crispy snack bar using colored rice, as the main ingredient. In this study, physicochemical properties of three rice varieties including Riceberry rice, Leum Phua glutinous rice, and RD6 sticky rice were compared. This study provided the development of crispy rice bar as healthier snack recipe and suggested for further utilization in prospective commercial grade.

2. Materials and methods

2.1 Materials

Raw materials include black glutinous rice (Leum Phua), white glutinous rice (RD6 rice), Riceberry rice, sunflower seeds, pumpkin seeds, cashew nuts, black sesame, white sesame, raisins, ripe banana (cv. Kluai Kai), glucose syrup, gum arabic, honey, brown sugar, salt, vegetable oil. Chemical reagents including ethanol, acetic acid, sodium acetate, potassium chloride, sulfuric acid, sodium hydroxide and 3,5-dinitrosalicylic acid were used in this study.

2.2 Experimental design

To develop nutritious snack bar with Thai rice mixed cereals, the sample of each type of rice varieties were conducted in Thailand. There were five experimental groups in this study, consisted of crispy rice product by Riceberry rice, black glutinous rice (Leum Phua), white glutinous rice (RD6), soaked white glutinous rice in water from black glutinous rice (soaked RD6 rice), and a combination of white and black sticky rice (combined RD6 with Leum Phua). Physicochemical and sensory test were evaluated.

2.3 Crispy rice formulation development

2.3.1 Crispy rice preparation with/without oil

RD6 glutinous rice was dried at 65º C. 10 g of dried RD6 was roasted without oil on pan fried at 270º C. Crispy rice characteristics in terms of rice seed inflation, color, odor and texture were observed after roasting the rice. Another dried RD6 (10 g) was fried at 230º C for 7 to 9 sec. Characteristic descriptions of crispy rice were noted. The effect of rice preparation with/without oil on product characters were reported.

2.3.2 Cereals preparation

Pumpkin seeds were roasted at 270º C for 10 min. Cashew nuts were roasted at 150º C for 15 min. Black and white sesame were roasted at

Suan Sunandha Science and Technology Journal

270º C for 7 min. All roasted cereals were packed in polyethylene bag.

2.3.3 Banana syrup preparation

Ripe bananas were cleaned and peeled. Banana pulps were sliced and mixed with water. The ratio of bananas and water was 1:1. Sliced banana was heated at 100º C for 5 min. Banana pulp was filter. The clear banana juice was heated at 80º C and further concentrated to 60 to 70º Brix. Banana syrup was contained in sterile bottles and stored at 4 to 5º C.

2.4 Crispy rice formulations

Standard formulation for crispy rice mixed cereals bar includes crispy rice 200 g, glucose syrup 160 g, Kluai Kai syrup 50 g, honey 60 g, brown sugar 50 g, salt 3 g, pumpkin seeds 30 g, sunflower seeds 30 g, white sesame 10 g, black sesame 10 g and raisin 50 g. Crispy rice and cereals were mixed and rested in the bowl for a while. Subsequently, glucose syrup mixed with Kluai Kai syrup were heated for 5 min. Honey, brown sugar and salt were added to mixed syrup and stewed for 2 min until the mixture was homogeneous. The mixture was poured into the bowl and immediately mixed with crispy rice and cereals. Then, look it cool down for 5 min and cut into small pieces with equal size (2.5×5×1 cm). Crispy rice mixed cereal bar were packed in polyethylene bag and stored at room temperature for further analysis.

2.5 Product quality analyses

2.5.1 Physical property of crispy rice bar

Color and water activity (a_w) were analyzed by a spectro-photo-colorimeter and LabMaster-A_w, respectively. Color value was expressed as L^*, a^* and b^*. Degree of whiteness or darkness were indicated by L^* (0 = black, 100 = white). Degree of redness (+) or greenness (-) were expressed as a^*. Yellowness (+) and blueness (-) scales were indicated as b^*. Water activity was expressed as the ratio of the vapor pressure in food to the vapor pressure of pure water. A texture analyzer (TA.XT.Plus) was used to measure the crispness.

2.5.2 Chemical property of crispy rice bar

Moisture content was determined by A.O.A.C method (1995). Reducing sugar was analyzed using dinitrosalicylic acid (DNS) method as previously described by James, C. S. (1995).

2.5.3 Quantification of total anthocyanin content

Total anthocyanin content was determined by pH differential method (modified from Lee *et al.*, 2005). Ethanol solvent at 70% was used to extract the anthocyanin. Absorbance was read at 510 nm in a spectrophotometer.

2.5.4 Organoleptic evaluation

Crispy rice sensory evaluation was obtained from 24 untrained panels by 9-point hedonic scale test. Color, odor, flavor, and texture as well as the overall liking were evaluated from extremely dislike as '1 point' to extremely like as '9 point'.

2.5.5 Product quality during storage

The final formula of crispy rice was selected by the highest sensory point for product quality analysis during storage for 2 months. The selected product was evaluated for color, lipid oxidation, and water activity as well as bacterial growth. Product was observed and reported at day 0, 15, 30 and 60.

2.6 Data analysis

All analyses were carried out in triplicate. The results were expressed as mean values and standard deviation (SD). The mean of three or more groups were analyzed for the statistically significant differences using one-way analysis of variance (ANOVA) and Duncan's Multiple Range Test (DMRT). Two-sided p-value < 0.05 were regarded as statistically significant. All statistical analyses were performed using Statistical Package for the Social Science (SPSS) 17.0 software.

3. Results and discussion

This study explored the effect of cooking process on quality characteristics of crispy rice by the comparison of frying with/without vegetable oil. The

Vol.07, No.1 DOI:10.14456/ssstj.2020.6

Suan Sunandha Science and Technology Journal

result showed that cooking oil influenced on crispy rice quality in terms of seed swelling, color, odor and texture. Crispy rice with cooking oil represented more pleasant product quality than crispy rice without cooking oil (Table 1). Fat and oil play important roles to food product. One of oil capacity is the heat absorption which is more effective than air or water. It transfers heat to rice seed surface as well as enhances color and texture of the crispy rice. It plays important role in food product which is responsible for developing texture and enhancing flavor of fried foods. In addition, oil penetrates and replaces water in food during frying, resulting in more tenderizing. Oil also releases ingredient flavor and produces moistness feeling in the mouth. (Oke et al., 2017) Hence, heating process with vegetable oil resulted in better characteristics in terms of crispness, desirable color and pleasing smell of the fried crispy rice while another cooking process was slightly burnt and hard. The crispy rice by optimum oil usage was considerably more acceptable

.

Table 1. Qualitative characteristics of crispy rice by heated with/ without vegetable oil

Rice characters	Without oil	With oil
Rice seed	Little inflated	More inflated
Color	Yellow-brown	Yellow-white
Odor	Burnt smell	Pleasing scent
Texture	Crisp with hard cracked	Crisp with easily cracked

Total anthocyanin contents in Leum Phua sticky rice and Riceberry rice were compared before the heating process and after food processes by drying and frying (Table 2). The result indicated that food processing affected on anthocyanins. Total anthocyanin content was high at raw and subsequently decreased during food process. Significantly, Leum Phua glutinous rice had higher anthocyanins than Riceberry rice at stage of raw material and after drying. However, total anthocyanin contents were no different between Riceberry rice and Leum Phua stucky rice after frying process. In fact, anthocyanin are easily oxidized during process and storage by several factors such as pH, light, and oxygen, as well as enzymes. One of the important factors to be considered is processing temperature. Anthocyanin stability was affected and degraded into various intermediate compounds by heat. (Patras *et al.*, 2010, pp. 3-11). The finding was consistent with Surh and Koh's study (2014) that presented higher anthocyanins at raw in two cultivars of black rice (*Oryza sativa* cv. Sintoheugmi and Sinnongheuchal). The large amount of anthocyanins were decreased after heat process, for example, roasting, pan-frying, steaming and boiling. As same as the study of Hiemori, Koh and Mitchell (2009) that revealed the degradation of total anthocyanins into the protocatechuic acid in cooking black rice (*Oryza sativa* L. *Japonica* var. SBR). Leum Phua and Riceberry rice showed total anthocyanins content in approximately 317.28 and 235.64 mg/100 g of rice, respectively (Table 2). The result was in range from previous study of Riceberry in different areas of Thailand which was 24.69-272.76 mg/100 g of rice (Settapramote et al., 2018).

Table 2. Comparison of total anthocyanins in Leum Phua and Riceberry rice after heat process

	Total anthocyanin content (mg/100 g of rice)		
	Raw	After drying	After frying
Leum Phua	5712.87± 1273.34^{a}	1384.15± 141.00^{a}	450.87± 28.92 ^{a}
Riceberry	669.81± 125.25^{b}	317.28± 130.43^{b}	235.64± 57.93^{a}

Values are shown as mean±standard deviation. Means within each column bearing different superscripts are significantly different ($p<0.05$).

Crispy rice product were fried using vegetable oil. All formulas were developed as shown in Figure 1. The brightness was observed in RD6 crispy rice, followed by soaked RD6, combined RD6 with Leum Phua, Riceberry rice, and Leum Phua sticky rice, respectively (Table 3). The highest redness and yellowness were also detected in RD6 formula. Obviously, pigmented rice as Riceberry and Leum Phua were expressed lower scale of brightness and increased blue and green colors. According to the finding by previous reports in Thailand, Leum Phua

Vol.07, No.1 DOI:10.14456/ssstj.2020.6

Suan Sunandha Science and Technology Journal

and Riceberry rice significantly presented the darkness color whereas RD6 sticky rice showed more brightness (Poomipak et al., 2018). It can be explained that anthocyanin accumulation in Leum Phua and Riceberry resulted in lower of brightness scale.

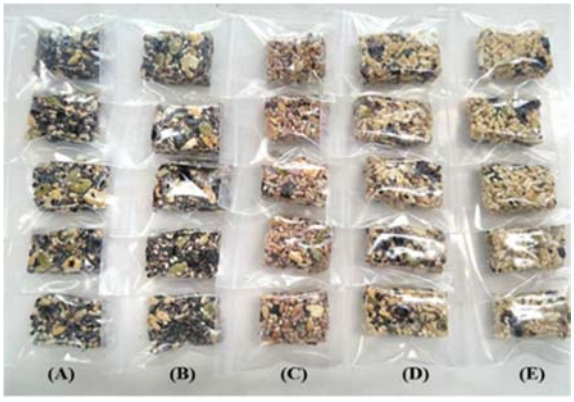

Figure 1. Crispy rice bar products (A) Leum Phua sticky rice, (B) Riceberry rice, (C) soaked RD6 in water from Leum Phua sticky rice, (D) combined RD6 with Leum Phua sticky rice, and (D) RD6 sticky rice

Table 3. Color scale of crispy rice products by different formulations

	Color scale		
	L*	**a***	**b***
Leum Phua	46.74±0.19^{c}	2.20±0.15^{d}	0.43±0.00^{e}
Riceberry	47.08±0.33^{c}	2.80±0.04^{c}	6.18±0.18^{d}
RD6 rice	54.69±0.80^{a}	5.12±0.18^{a}	16.64±0.31^{a}
Combined RD6 with Leum Phua	51.92±0.70^{b}	3.86±0.07^{b}	12.30±0.01^{b}
Soaked RD6 in water from Leum Phua	54.26±0.57^{a}	4.11±0.20^{b}	11.00±0.04^{c}

Values are shown as mean±standard deviation. Means within each column bearing different superscripts are significantly different ($p<0.05$).

Reducing sugar, moisture, and free water as well as texture were reported in Table 4. There was no significant difference of moisture and texture among groups. Factors affecting the textural quality of crispy rice snack include amylose content and moisture content. Amylose molecules are aligned by hydrogen bonds and release water molecules. However, the RD6, riceberry and Leum Phua are the rice with very low amylose content (5-12%) (Boonmeejoy et al., 2019). Thus, the moisture content and crispness were not difference in this study. The higher amount of reducing sugar was found in combined RD6 with Leum Phua, followed by soaked RD6, RD6, Riceberry, and Leum Phua glutinous rice, respectively. The reducing sugar of formulations with RD6 sticky rice were likely to be high because white glutinous rice had higher starch digestibility than colored rice varieties. Therefore, increasing amount of reducing sugar can be imply to degradation of the starch during the process (Pasakawee et al., 2018). The lowest free water in product was observed in both Riceberry and soaked RD6 formulas with water activity 0.41. All formulations were within the range 0.41-0.44 which reaction rate was low for undesirable microorganism growth, browning, and enzyme activity (Sandulachi, 2003).

Table 4. Reducing sugar, moisture content, water activity and texture of crispy rice product by different formulations

	Reducing sugar (g/ml)	**Moisture (%)**	**Free water**	**Crispness (N)**
Leum Phua	12.91	7.08± 0.30^{a}	0.43± 0.00^{a}	51.54± 26.02^{a}
Riceberry	13.02	7.05± 0.42^{a}	0.41± 0.00^{b}	63.73± 33.23^{a}
RD6 rice	13.11	7.22± 0.57^{a}	0.42± 0.00^{a}	75.34± 60.71^{a}
Combined RD6 with Leum Phua	13.56	7.07± 0.25^{a}	0.42± 0.00^{a}	38.05± 17.39^{a}
Soaked RD6 in water from Leum Phua	13.22	6.77± 0.21^{a}	0.41± 0.00^{b}	61.55± 21.13^{a}

Values are shown as mean±standard deviation. Means within each column bearing different superscripts are significantly different ($p<0.05$).

Mean of total anthocyanin contents were compared by various formulations as shown in Figure 2. Total anthocyanins significantly differed

Suan Sunandha Science and Technology Journal

between pigmented rice and pure RD6 sticky rice. There was no significance difference among Riceberry rice, combined RD6 and soaked RD6 formulations. Additionally, Leum Phua crispy rice had the highest total anthocyanin content (371.09±11.58 mg/100g), followed by Riceberry (144.72±16.70 mg/100g), combined RD6 with Leum Phua (128.02±25.51 mg/100g), soaked RD6 (122.46±22.27 mg/100g), and RD6 sticky rice (87.21±47.99), respectively. Notably, colored rice, particularly Leum Phua was represented as the rich source of anthocyanins. In this sense, the previous study additionally supported that Leum Phua and Riceberry rice had higher phenolic compounds and scavenging ability than white glutinous rice, RD6 (Poomipak et al., 2018).

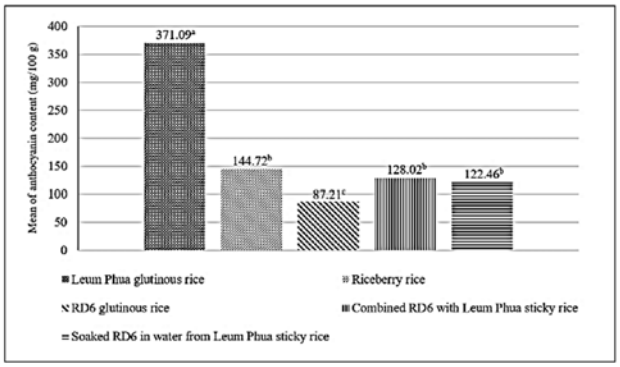

Figure 2. Mean of anthocyanins content in crispy rice products by different formulations

All formulations were ranked score from 1-9 in terms of color, odor, flavor, texture, and overall liking. There was no significant difference in odor, flavor, texture, and overall liking among groups. RD6 and soaked RD6 rice were obtained higher score in color and the highest score was found in soaked RD6 formula (Table 5). The lower score was observed in product with dark color by pigmented rice as based-material. The sensory test was inconsistent with previous study by Poomipak *et al.* (2018, pp. 134-143). They showed that unpolished Leum Phua sticky rice had higher scores in color. However, in this present, color score of developed sticky rice was high in RD6 and soaked RD6 formula. This may be explained by difference of age duration of panelists between the studies. Thus, the desirable formula of crispy rice product for consumers was made from soaked RD6 rice in Leum Phua's water sticky rice. Subsequently, the selected product was analyzed for proximate composition and quality during storage life. Moisture, protein, fat, ash and carbohydrate were 6.77, 681, 16.05, 0.73, and 69.64%, respectively (data not shown).

Table 5. Means sensory scores of crispy rice products by different formulations

	Leum Phua	Rice berry	RD6 rice	Combined RD6 with Leum Phua	Soaked RD6 in water from Leum Phua
Color	6.25±1.73^{b}	6.83±1.63^{b}	7.21±1.02^{a}	6.46±1.59^{b}	7.42±0.93^{a}
Odor^{ns}	6.38±1.38	6.08±1.38	6.13±1.26	6.42±1.53	6.46±1.18
Flavor^{ns}	6.30±1.55	6.46±1.35	6.33±1.34	6.42±1.25	6.58±1.21
Texture^{ns}	5.38±1.93	6.13±1.62	6.08±1.79	5.88±1.78	6.08±1.50
Overall liking^{ns}	6.17±1.46	6.42±1.50	6.33±1.27	6.58±1.21	6.46±1.30

Values are shown as mean±standard deviation. Means within each column bearing different superscripts are significantly different ($p<0.05$). ns means no significant difference.

Table 6. Color analysis of crispy rice (soaked RD6 rice formula) during storage for 2 months

	Color scale		
	L*	a*	b*
Day 0	51.92±1.73^{a}	3.86±0.08^{a}	12.30±0.32^{a}
Day 15	51.80±2.82^{a}	3.82±0.03^{a}	12.70±0.12^{a}
Day 30	49.67±2.08^{a}	3.43±0.11^{b}	17.04±0.23^{b}
Day 60	48.25±2.76^{a}	3.04±0.06^{c}	17.19±0.37^{b}

Values are shown as mean±standard deviation. Means within each column bearing different superscripts are significantly different ($p<0.05$).

Product quality was measured after storage for 2 months at day 0, 15, 30, and 60. The scale of product color had been changing during storage at room temperature. Yellowness was increase while brightness and redness were decrease (Table 6). This phenomenon can be explained by browning reaction due to the increase of available water and lipid oxidation during storage. Non-enzymatic browning

Vol.07, No.1 DOI:10.14456/ssstj.2020.6

Suan Sunandha Science and Technology Journal

is occurred by the interaction of reducing sugars and amino acids. This reaction further to amadori compounds and form dark pigments. It causes of the quality change in food product due to darkening of light colored product (Singh & Anderson, 2004).

Malondialdehyde and thiobituric acid (TBA) reactivity was used as an index of lipid peroxidation. Lipid peroxidation and water activity were observed during the storage for 2 months (Figure 3). The increase of water activity and lipid peroxidation were detected. Water activity was not significant difference among periods. Noticeably, at day 60, the TBA value was significantly higher than day 0 and 15. Lipid oxidation is affected by light, oxygen, water activity and temperature as well as material composition. The snack formula included cereals as the main ingredient and using cooking oil for food process. Lipid reactions are catalyzed by both of non-enzymatic and enzymatic involvement which presenting in cereal components such as its membrane structure. Additionally, water content in mature grain and food processing also affected the lipid mobility and promoted reactions between lipids and other ingredients. Moreover, free fatty acids in rice and subsequently lipid oxidation products is partially attributed to storage under warm and humid conditions even the lipid content of rice is slightly low. Thus, crispy rice stored in laminated bags containing CO_2 or under refrigerated conditions were likely to be more stable than stored at ambient temperature (Lehtinen, 2003; Angelo et al., 2009,). Similar results were reported by previous study (Thaweeseang et al., 2017) that showed ongoing increase of TBA value and water activity in nutritious cereal bar during the 30 days storage. However, in this study, the TBA value was in range 0.34-0.53 within 2 months that was lower than acceptance limit for rancidity (1.0 mg/kg).

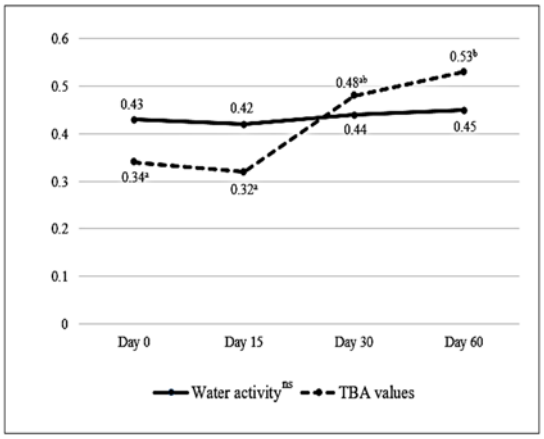

Figure 3. Means of water activity and TBA values (mg MDA/kg) in crispy rice product (the soaked RD6 formula) during storage for 2 months. The values with different superscript letters mean significantly different ($p<0.05$). ns means no significant difference.

Table 7. Bacterial count of crispy rice product (soaked RD6 formula) stored at 25º C for 2 months

	Day 0	Day 15	Day 30	Day 60
Total bacterial count (CFU/g)	<10	<10	2.5×10	1.26×10^2
Yeast and moulds (CFU/g)	<10	<10	<10	<10
Coliform bacteria (MPN/g)	ND	ND	ND	ND
Staphylo-coccus aureus (MPN/g)	ND	ND	ND	ND
Escherichai coli (MPN/g)	ND	ND	ND	ND

ND-Not detected

The crispy rice products of the RD6 soaking with water from black glutinous rice were examined for microbiology count on days 0, 15, 30, and 60. Total bacterial count was below 10 at day 0 and 15. The spoilage were observed at the 30th and 60th storage day but not beyond the standard range. This result was supported by the increase of water activity during the storage period. Yeast and mould were lower than 10 CFU/g through the study. In addition, there was no growth of Coliform bacteria, Staphylococcus aureus, and E. coli during 2 months

Vol.07, No.1 DOI:10.14456/ssstj.2020.6

of storage (Table 7). Hence, the product was microbiologically safe within 2 months of storage period at room temperature.

4. Conclusion

In this study, cooking process with vegetable oil resulted in the desirable quality of the crispy rice product. According to this result, five formulations, including black glutinous rice (Leum Phua), Riceberry rice, white glutinous rice (RD6), RD6 soaking in water from Leum Phua sticky rice, and combined RD6 with Leum phua sticky rice were developed to high anthocyanin snack bar by frying method. The anthocyanin from black rice was high at raw and subsequently decreased during the heating process. Obviously, Leum Phua crispy rice had the highest anthocyanin, followed by Riceberry rice. However, the color of pigmented rice affected the sensory scores. Low brightness of product was associated with lower score. The RD6 soaking in water from Leum Phua represented as the final product formula of crispy rice bar due to high anthocyanin and acceptable sensory score. Therefore, it can be concluded that crispy rice bar from glutinous rice and glutinous rice RD6 soaking with black glutinous rice are suitable for commercial production because it can increase the nutrition value for consumers by providing high anthocyanin content. Moreover, the RD6 crispy rice soaking in water from black glutinous rice was be able to store up to 2 months of storage.

5. Acknowledgement

This research was supported by Institute of Food Research and Product Development (IFRPD), Kasetsart University.

6. Publication Ethic

Submitted manuscripts must not have been previously published by or be under review by another print or online journal or source.

7. References

Angelo, A. J. St., Vercellotti, J., Jacks, T., & Legendre, M. (2009). Lipid oxidation in foods. *Critical Review in Food Science and Nutrition, 36*(3), 175-224. doi: 10.1080/10408399609527723

AOAC. (1995). Official methods of analysis of AOAC international. In T. R. Mulvaney (Ed.), *AOAC International* (p. 42-1-42-2). Arlington, VA.

Boonmeejoy, J., Wichaphon, J., & Jiamyangyuen, S. (2019). Classification of rice cultivars by using chemical, physicochemical, thermal, hydration properties, and cooking quality. *Food and Applied Bioscience Journal, 7*(2), 42-62.

James, C.S. (1995). *Analytical chemistry of food*. Seale-Hayne faculty of agriculture, university of Polymouth, UK.

Khoo, H. E., Azlan, A., Tang, S. T., & Lim, S. M. (2017). Anthocyanidins and anthocyanins: colored pigments as food, pharmaceutical ingredients, and the potential health benefits. *Food and Nutrition Research*, *61*(1),1-22. doi:10.1080/16546628.2017.1361779

Lee, J., Durst, R. W., & Wrolstad, R. E. (2005). Determination of total monomeric anthocyanin pigment content of fruit juices, beverages, natural colorants, and wine by the pH differential method: Collaborative study. *Journal of AOAC International*, *88*(5), 1269-1278.

Lehtinen, P. (2003). *Reactivity of lipids during cereal processing* (Doctoral thesis). Helsinki University of Technology. Finland.

Hiemori, M., Koh, E., & Mitchell, A. E. (2009). Influence of cooking on anthocyanins (*Oryza sativa* L. *japonica* var. SBR). *Journal of Agriculture and Food Chemistry, 57*(5), 1908-1914. doi: 10.1021/jf803153z.

Suan Sunandha Science and Technology Journal

Ngamdee, P., Bunnasart, A., & Sonda, A. (2019). Development of a functional food: milk chocolate fortified with anthocyanin from broken Riceberry. *Rajabhat Journal of Sciences, Humanities & Social Sciences, 20*(1), 81-89.

Oke, E. K., Idowu, M. A., Sobukola, O. P., Adeyeye, S. A. O., & Akinsola, A. O. (2017). Frying of food: a critical review. *Journal of Culinary Science & Technology,* 1-21. doi:10.1080/15428052.2017.1333936

Pasakawee, K., Laokuldilok, T., Srichairatanakool, S., & Utama-ang, N. (2018). Relationship among starch digestibility, antioxidant, and physicochemical properties of several rice varieties using principal component analysis. *Current Applied Science and Technology, 18*(3), 1-12.

Patras, A., Brunton, N. P., Donnell, C. O., & Tiwari, B. K. (2010). Effect of thermal processing on anthocyanin stability in foods; mechanisms and kinetics of degradation. *Trends in Food Science & Technology, 21*(1), 3-11. doi: 10.1016/j.tifs.2009.07.004

Poomipak, N., Samakradhamrongthai, R. S., Utama-ang, N. (2018). Consumer survey of selected Thai rice for elderly using focus group and acceptance test. *Food and Applied Bioscience Journal, 6* (special issue on food and applied bioscience), 134-143.

Sandulachi, E. (2003). Water activity concept and its role in food preservation. In, Mrema, G. C. (Eds.), *Handling and preservation of fruits and vegetables by combined methods for rural areas* (pp. 40-48). Rome: Food and Agriculture Organization of the United Nations.

Settapramote, N., Laokuldilok, T., Boonyawan, D., & Utama-ang, N. (2018). Physicochemical, antioxidant activities and anthocyanin of Riceberry rice from different locations in Thailand. *Food and Applied Bioscience Journal, 6*(special issue on food and applied bioscience), 84-94.

Singh, R. P., & Anderson, B. A. (2004). The major type of food spoilage: An overview. In Steele, R. (Ed.), *Understanding and measuring the shelf-life of food* (p. 3-23). Aspen Publications, Gaithersburg, MD.

Sirichokworrakit, S., Phetkhut, J., & Khommoon, A. (2015). Effect of partial substitution of wheat flour with Riceberry flour on quality of noodles. *Procedia- Social and Behavioral Sciences, 197*,1006- 1012. doi: 10.1016/j.sbspro.2015.07.294

Sivamaruthi, B. S., Kesika, P., & Chaiyasut, C. Anthocyanins in Thai rice varieties: distribution and pharmacological significance. *International Food Research Journal, 25*(5), 2042-2032.

Surh, J., & Koh, E. (2014). Effects of four different cooking methods on anthocyanins, total phenolics and antioxidant activity of black rice. *Journal of the Science of Food and Agriculture, 94*(15), 1-9. doi: 10.1002/jsfa.6690

Suwannalert, P., & Rattanachitthawat, S. (2011). High levels of phytophenolics and antioxidant activities in Oryza sativa-unpolished Thai rice strain of Leum Phua. *Tropical Journal of Phamaceutical Research*, *10*(4), 431-436. doi:10.4314/tjpr.v10i4.8

Thaweeseang, N., Katakul, S., Sreela-or, C. (2017). Product development of nutritious cereal bar. *Rajamangala University of Technology Srivijaya Research Journal, 9*(2), 212-223.

Available online at http://www.ssstj.sci.ssru.ac.th

SSSTJ

Suan Sunandha Science and Technology Journal

Promotion of Community Participation for Saline Soil Remediation by Alternative Technology of Bio-Organic Fertilizers and Nano Material at Krabueang Yai, Phimai District, Nakhon Ratchasima Province

Waraporn Kosanlavit*, Bupachat Tobunsung , Napat Noinumsai

Faculty of Science and Technology, Nakhon Ratchasima Rajabhat University,
Nakhonratchasima 30000, Thailand

Corresponding author e-mail: * waraporn.k@nrru.ac.th, waraporn.kslvit@gmail.com

Received: *19 December, 2019* / **Revised:** *10 January 2020* / **Accepted:** *17 January 2020*

Abstract

This paper is applied research to create changes in the community. The objectives of this research were the study of the bio-organic fertilizer production process in Ban-Toey Community Enterprise at Krabueang Yai, Phimai District, Nakhon Ratchasima Province and promoting the community participation in the remediation of saline soil by the alternative technology such as bio-organic fertilizers and nanomaterial. The research methodology of this study was carried out by studying the data sources and information from the community and on-site events or activities Moreover, in-depth interviews, group discussions, observation, questionnaires, demonstrations were also carried out in order to transfer knowledge from the laboratory outcome to the community. The result was found that promotion of community participation for saline soil remediation by alternative technology of bio-organic fertilizers and nanomaterials at Krabueang Yai were operated by share and learn activities, in-depth interviews, group discussion, observation and questionnaires. The demonstrations were also carried out in order to transfer knowledge from the laboratory outcome to the community. After the activities, it was found that the community changes including a deep understanding of the saline soil solutions, production of bio-organic fertilizer, nanotechnology and soil tests. Moreover, Ban-Toey villagers planned to establish soil quality analysis services during the soil adjustment of the field and agricultural area. A cooperative creating was to resolve saline soil problems. In addition, the view of the participants should be changed that nanomaterial could be non-expensive. Participants who were more liberal on new ideas such as nanotechnology can be the better starting point for the solving of saline soil problems and alternatively helping the community to increase agricultural productivity and benefits.

Keywords: Community participation, Saline soil, Alternative technology, Bio-organic fertilizers, Nanomaterial

1. Introduction

Currently, there are new technologies and that can be applied to solve the problems in agriculture including soil quality improvement. One of the technologies is nanotechnology which is used as a better alternative. Nanotechnology is the technology that involves the process of managing, creating, or analyzing of small materials in nanometer (about 1-100 nm) (El-Shall, Graiver, Pernisz, & Baraton, 1995; Masciangioli & Zhang, 2003). Nano-sized particles are applied in environmental applications such as applying in treatment and improvement of the environmental contaminations in soil, water, and air (Jiamjitrpanich, Parkpian, Polprasert, & Kosanlavit, 2012, 2013; Jiamjitrpanich, Parkpian, Polprasert, Laurent, & Kosanlavit, 2012; Jiamjitrpanich, Polprasert, Parkpian, Delaune, & Jugsujinda, 2010). Nanoscale Carbon (nC) is a special element that can be found in many allotropic forms and also it is used in cell culture, biosensors, and can be applied in the environment by being used as adsorbents, filters, water filters, conductor, gas sensors. Moreover, it can used in wastewater treatment, air pollution treatment, etc. In addition, it is environmentally friendly. Bio-Organic Fertilizer (BOF) is an organic fertilizer that has been processed at high temperatures. This process can kill microbes which are causes of plant disease, animal and human disease, as well as general microbes. After that, microorganisms which have fertilizer properties are added to this kind of fertilizer. They help to fix nitrogen for plants and to produce plant hormones to stimulate the growth of plant roots. Also, some microbes can control plant diseases in the soil and stimulate an immunity production of plants. (Department of Land Development, 2013). Krabueang Yai Subdistrict Community, Phimai District, Nakhon Ratchasima

Suan Sunandha Science and Technology Journal

Province the groups of farmers established and trained to produce bio-organic fertilizer in the community.

So, this research is interesting as it was applied the bio-organic fertilizer which produced by the Ban Toey village community, Krabueang Yai, Phimai District, Nakhon Ratchasima Province in combination with nanoparticles to saline soil rehabilitation. Rice is mainly grown in this area, thus rice husk is used as a saline soil improvement material (soil amendment) both fresh rice husk and rice husk ash. Soil amendment means any material that is put into the soil for improve soil properties to suitability in crop cultivation but not used as a substitute for fertilizer or as fertilizer. Soil amendment can divided into 2 types; 1) Material for physical soil improvement, it will help to make the soil coarse structure, water drainage and airflow in the soil will be improved such as rice husk, sawdust, manure, compost, crop residue, and various polymers. 2) Material for chemical soil improvement, it will help adjust soil pH to increase the absorb ability of plant nutrients; reduce the toxicity of toxic elements in soil.

Therefore, the solving of saline soil problems in Krabueang Yai Community, Phimai District. Nakhon Ratchasima Province which is located on the Korat salt basin and has a rock salt causing problems in salinity spreading, thus this research applied modern technology including nanotechnology combined with local wisdom including bio-organic fertilizer used to reduce salinity in the soil. Also, the process of community participation was used to solve the saline soil problems and achieve sustainable development.

2. Objectives

2.1 To study the production of bio-organic fertilizer of Ban Toey Community Enterprise, Krabueang Yai Subdistrict, Phimai District, Nakhon Ratchasima Province.

2.2 To develop and promote the community participation in the rehabilitation and resolution of saline soil problems with alternative technologies.

3. Scope of research

Conceptual framework consists of concepts, goals and concrete of the things that need to be driven to see results within the time period of operation as shown in Figure 1.

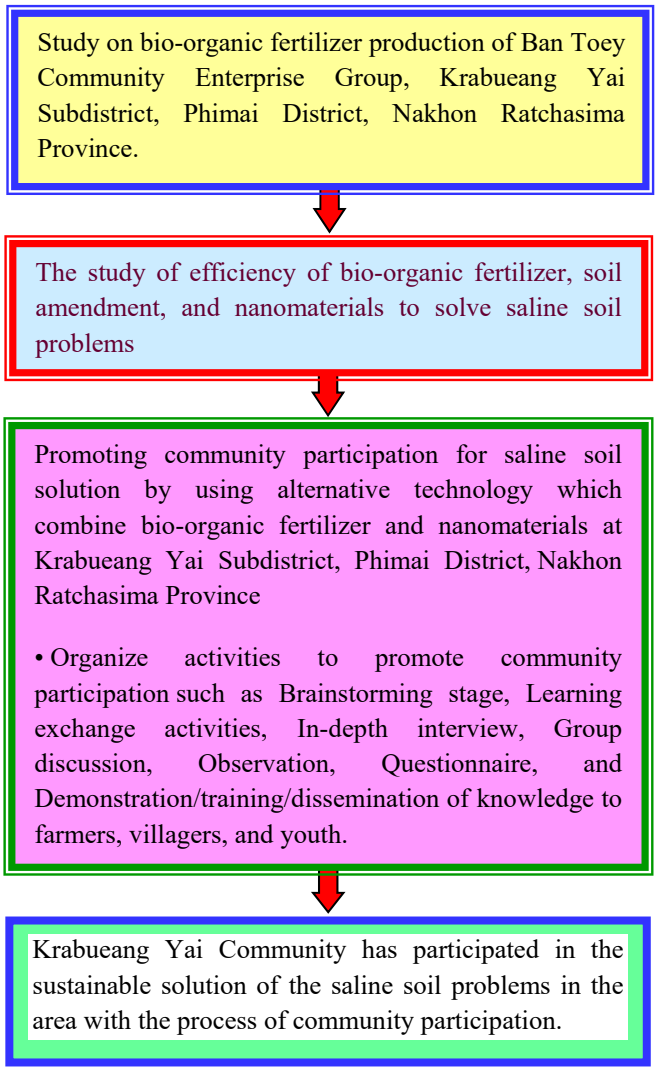

Figure 1. Research conceptual.

4. Methodology

4.1 Study area

Promoting community participation for salt soil solution by using alternative technology of integration of bio-organic fertilizer and nanomaterials are studied at Krabueang Yai Subdistrict, Phimai District, Nakhon Ratchasima Province.

4.2 Population and sample groups of this study

A population is a group of farmers and villagers in the saline soil problem areas at Krabueang Yai Subdistrict, Phimai District, Nakhon Ratchasima Province. The sample groups are farmers and villagers in the salt soil area at Krabueang Yai Subdistrict, Phimai District, Nakhon Ratchasima Province by specific sampling in the

Vol.07, No.1 DOI: 10.14456/ssstj.2020.7

problematic saline soil area, there were 181 persons.

4.3 Data collection

The research methodology of this paper was divided into 2 parts according to the objectives, which could be implemented as follows:

Part 1: Study of bio-organic fertilizer production of Ban Toey Community Organic Bio-fertilizer, Phimai District, Nakhon Ratchasima Province by interviewing members and community leaders and study the production process of bio-organic fertilizer of community enterprise groups.

Part 2: Promoting community participation for saline soil solution by using alternative technology of integration of bio-organic fertilizer and nano-materials.

Organizing of learning exchange activities, in-depth interviews, group discussions, brainstorming ideas, observing activities, demonstration/knowledge dissemination from research knowledge to the community to solve the saline soil problem in the study area. Also, the organization of learning and exchanging activities among communities, local scholars, researchers, and students were divided into 4 learning bases: Learning base I Saline soil and soil analysis, Learning base II Nanotechnology and environment, Learning base III Bio-organic fertilizer (Ban Toey), and Learning base IV Combining bio-organic fertilizer, nanomaterials and soil amendments to solve saline soil problems. A learning base operated by the community had a role to demonstrate/train/disseminate knowledge to the community (farmer groups and youth).

4.4 Tools used in research studies

(1) Questionnaire, interview and group discussion used as a tool to study community contexts and community problems caused by the saline soil area.

(2) Questionnaire, interview and group discussion used as a tool to study community participation in soil rehabilitation and saline soil problem solving before and after the project implementation.

(3) Specific interviews used as a tool to study the production of bio-organic fertilizer of Ban Toey community enterprise groups.

(4) Scientific equipment in the laboratory was used to study the effectiveness of saline soil reduction of bio-organic fertilizer, soil amendment and nanomaterials. Also, they were used to study the quality of saline soil before and after remediation.

4.5 Data analysis

(1) The study of the community context and the problems of the communities caused by the saline soil conditions and the community participation in the rehabilitation and solution of saline soil problems analyzed by descriptive statistics, average and standard deviation (SD).

(2) Soil quality data analyzed by descriptive statistics, average and standard deviation (SD).

5. Results and Discussion

Promoting the community participation for saline soil solutions by using alternative technology which integrates between bio-organic fertilizer and nanomaterials at Krabueang Yai Subdistrict, Phimai District, and Nakhon Ratchasima Province is an applied research. The results had 2 parts as shown below:

5.1 Bio-organic fertilizer production of Ban Toey community

The study of bio-organic fertilizer production of Ban Toey Community, Krabueang Yai Subdistrict, Phimai District, Nakhon Ratchasima Province conducted by interviewing members and community leaders of Ban Toey and Bio-organic fertilizer community enterprise groups.

Figure 2. Ban Toey bio-organic fertilizer production methods and community enterprise group interviews.

The study of bio-organic fertilizer production of Ban Toey Community by studying the specific formula and the process of production of bio-organic fertilizer of Ban Toey Community by interviewing members and community leaders of fertilizer manufacturer's community groups found that the formula of Ban Toey bio-organic fertilizer consists of 200 kg of animal manure, 100 kg. of molasses, 50 kg. of rice bran, 50 kg. of sugarcane ash, 100 kg bat guano and 80 liters of EM. Mix all ingredients together put into a blender

and using EM as a binder. Production capacity is 200 tons/year for self-use and distribution to members and general villagers.

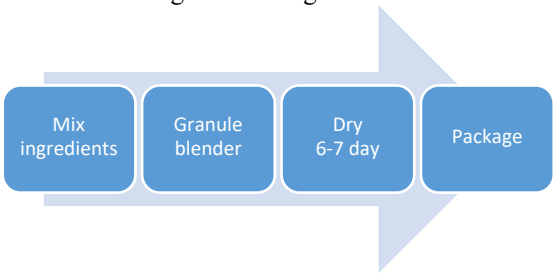

Figure 3. Ban Toey bio-organic fertilizer production diagram.

Figure 4. Ban Toey Bio-Organic Fertilizer Community Enterprise Group.

In addition, the results from in-depth interviews of the Ban Toey bio-organic fertilizer community group found that the fertilizer producer group had developed improve production formulas by constantly changing the ingredients and raw materials in EM production. Community enterprise group had divided duties and responsibilities that consist of a president, secretary, vice president, marketing, accounting, labor and public relations, procurement, inspection, and consultancy department as shown in Figure 8.

5.2 Promoting of community participation

Promoting of community participation in solving saline soil problems by using alternative technology to combine bio-organic fertilizer and nano-material.

5.2.1 Educational exchange activities, in-depth interviews, group discussion to brainstorm ideas, observation, demonstration activities /disseminating knowledge from the research to the community to solve the problem of saline soil in the area was organized. In this activities exchanging knowledge between communities, local scholars, researchers, and students had divided into 4 learning bases: Learning base I: Saline soil and soil analysis, Learning base II: Nanotechnology and environment, Learning base III: Bio-organic fertilizer (Ban Toey), and Learning base IV: Combining bio-organic fertilizer, nanomaterials and soil amendments to solve saline soil problems.

Figure 5. Learning base of activities to exchange knowledge and transfer knowledge.

By allowing the community to play a role in demonstrating/disseminating knowledge to the community (farmers, villagers and youth groups), the activity results showed that:

Learning base I: Saline soil and soil analysis.

Figure 6. Learning base I: Saline soil and soil analysis.

The base I: saline soil and soil analysis to this exchange of knowledge was a base for lecturing and discussing knowledge of saline soil, included the cause, the impact and the approach to the saline solution. In addition, there was the discussion activity and talk about experiences related to saline soil problems and solutions. Also, there were demonstration activities for soil quality analysis

methods including EC values (salinity indicator), pH values, nitrogen, phosphorus, and potassium. From the activities in this learning base, it was found that participants are interested in the content and get practicing tests to analyze the soil collected by themselves. There was also a suggestion and demand in the group discussions that wanted to have the basic equipment in villages and a service unit to analyze the soil quality in the next period before the soil preparation. From the discussion of the participants' ideas and experiences, including questionnaires, it was found that the saline soil problem in the past was more severe than present.

Nowadays, the saline soil problem has caused by the water source that flows passing from the salt field and caused by using a lot of chemical fertilizer. Participants suggested some methods to solve the problem such as adding compost, animal manure, green manure, vetiver grass, leaf scraps, mulching (ground cover), fresh rice husk, and plowing. Moreover, the participants mentioned creating a network and cooperating together in solving the saline soil problems.

Learning base II: Nanotechnology and environment.

Figure 7. Learning base II: Nanotechnology and environment.

Base 2: Nanotechnology and the environment was a base for exchanging knowledge that gives lectures and basic knowledge about nanotechnology for participants to know about nanotechnology and nanomaterials application. Nanotechnology in environmental work is using for treatment soil, water, air, and water pollution. Nanotechnology is used to promote agricultural work, cultivation, disease and various pathogens management. It was found that 54 percent of the participants knew nanotechnology or nano-fertilizer, and 46 percent do not know, mostly they known only the names and properties of the advertisement, but not truly understood meaningful and have never been used. The activities in this base received a lot of interest and questions from the participants. This activity makes the participants more understand about nanotechnology. In addition, the researchers found that the mindsets of the participants had changed that nanomaterials must have expensive; on the other hand, nanomaterials are many types and the price are vary (cheap to expensive). They could accept nanotechnology to be used to solve saline soil problems and help them to increase productivity as well.

Learning base III: Bio-organic fertilizer (Ban Toey).

Figure 8. Ban Toey bio-organic fertilizer.

Base 3: Ban Toey bio-organic fertilizer was a base for learning about bio-organic fertilizer production of groups of Ban Toey bio-organic fertilizer community enterprise which the members of the enterprise group were invited as speakers to give lectures on production knowledge and experience to participants (groups of villagers, leaders, communities, and students). It was found that participants get knowledge of the process of the products and ingredients. Participants are interested to try to make their fertilizer and ask to contact the Ban Toey bio-organic fertilizer community enterprise group for solving the problem of saline soil.

Learning base IV: Combining bio-organic fertilizer, nanomaterials, and soil amendments to solve saline soil problem

Figure 9. Learning base IV: Combining bio-organic fertilizer, nanomaterials, and soil amendments to solve saline soil problems.

Learning base 4: Combining bio-organic fertilizer, nanomaterials and soil amendments to solve saline soil problems was a learning base that using knowledge from the results of the research on the study of the effectiveness of organic nano-biological fertilizer to solve saline soil problems which this research combines Ban Toey bio-organic fertilizer with nano-carbon material and soil amendment (fresh rice husk and rice husk ash) used to improve saline soil. From organizing activities in this base, it was found that the participants transferred the knowledge gained from research and they were interest in the use of knowledge to solve saline soil.

6. Conclusion

Krabueang Yai Subdistrict area is an area experiencing saline soil problems due to the Korat salt basin. It was found that community leaders and general participants had various activities for solving saline soil problems. They tried to solve the problem by using bio-organic fertilizer, compost, rice husk, and soil amendment and reducing chemicals fertilizers. Moreover, this research project helped establishing a unit for soil quality analysis before cultivation. The community created cooperation to solve saline soil problems between villages. The participants encouraged to using nano-bio-organic fertilizer as an alternative to solving the saline soil problems and increasing agricultural productivity.

7. Acknowledgement

This research received research funding from the Thailand Research Fund (TRF).

8. References

Department of Land Development. (2013). Salty tolerant plants and salt-like plants. [Online]. Department of Land Development. Retrieved from http: www. Idd.go.th. (25 August 2013).

El-Shall, M. S., Graiver, D., Pernisz, U., & Baraton, M. I. (1995). Synthesis and characterization of nanoscale zinc oxide particles: I. laser vaporization / condensation technique. *Nanostructured Materials*, *6*, 297-300.

Jiamjitrpanich, W., Parkpian, P., Polprasert, C., & Kosanlavit, R. (2012). Enhanced phytoremediation efficiency of TNT-contaminated soil by nanoscale zero valent iron. *International Proceedings of Chemical, Biological and Environmental Engineering*, *35*, 82-86.

Jiamjitrpanich, W., Parkpian, P., Polprasert, C., & Kosanlavit, R. (2013). Trinitrotoluene and its metabolites in shoots and roots of *Panicum maximum* in nano-phytoremediation. *International Journal of Environmental Science and Development*, *4*(1), 7-10.

Jiamjitrpanich, W., Parkpian, P., Polprasert, C., Laurent, F., & Kosanlavit, R. (2012). The tolerance efficiency of *Panicum maximum* and *Helianthus annuus* in TNT-contaminated soil and nZVI-contaminated soil. *Journal of Environmental Science and Health, Part A: Toxic / Hazardous Substances and Environmental Engineering*, *47*(11), 1506-1513.

Suan Sunandha Science and Technology Journal

Jiamjitrpanich, W., Polprasert, C., Parkpian, P, Delaune, R. D., & Jugsujinda, A. (2010). Environmental factors influencing remediation of TNT-contaminated water and soil with nanoscale zero valent iron particles. *Journal of Environmental Science and Health, Part A: Toxic / Hazardous Substances and Environmental Engineering*, *45*(3), 263-274. doi: 10.1080/10934520903468012

Masciangioli, T. & Zhang, W.-X. (2003). Environmental technologies at the Nanoscale. *Environmental Science & Technology*, *37*(5), 102-108. doi: 10.1021/es0323998